AEDC-TR-74-110

EVALUATION OF A WEDGE ON A FORCE BALANCE AS A FLOW ANGLE PROBE

H. Maxwell and W. Luchuk
ARO, Inc.

PROPULSION WIND TUNNEL FACILITY
ARNOLD ENGINEERING DEVELOPMENT CENTER
AIR FORCE SYSTEMS COMMAND
ARNOLD AIR FORCE STATION, TENNESSEE 37389

February 1975

Final Report for Test Conducted on January 29, 1974

Approved for public release; distribution unlimited.

Prepared for

DIRECTORATE OF TECHNOLOGY
ARNOLD ENGINEERING DEVELOPMENT CENTER
ARNOLD AIR FORCE STATION, TENNESSEE 37389

NOTICES

APPROVAL STATEMENT

This technical report has been reviewed and is approved for publication.

FOR THE COMMANDER

Lamar R. Kissling

LAMAR R. KISSLING
Lt Colonel, USAF
Chief Air Force Test Director, PWT
Directorate of Test

Frank J. Passarello

FRANK J. PASSARELLO
Colonel, USAF
Director of Test

REPORT DOCUMENTATION PAGE		READ INSTRUCTIONS BEFORE COMPLETING FORM
1. REPORT NUMBER AEDC-TR-74-110	2. GOVT ACCESSION NO.	3. RECIPIENT'S CATALOG NUMBER
4. TITLE (and Subtitle) EVALUATION OF A WEDGE ON A FORCE BALANCE AS A FLOW ANGLE PROBE		5. TYPE OF REPORT & PERIOD COVERED Final Report - January 29, 1974
		6. PERFORMING ORG. REPORT NUMBER
7. AUTHOR(s) H. Maxwell and W. Luchuk, ARO, Inc.		8. CONTRACT OR GRANT NUMBER(s)
9. PERFORMING ORGANIZATION NAME AND ADDRESS Arnold Engineering Development Center Arnold Air Force Station, Tennessee 37389		10. PROGRAM ELEMENT, PROJECT, TASK AREA & WORK UNIT NUMBERS Program Element 64719F
11. CONTROLLING OFFICE NAME AND ADDRESS Arnold Engineering Development Center (DYFS), Arnold Air Force Station, Tennessee 37389		12. REPORT DATE February 1975
		13. NUMBER OF PAGES 67
14. MONITORING AGENCY NAME & ADDRESS(if different from Controlling Office)		15. SECURITY CLASS. (of this report) UNCLASSIFIED
		15a. DECLASSIFICATION/DOWNGRADING SCHEDULE N/A

16. DISTRIBUTION STATEMENT (of this Report)

Approved for public release; distribution unlimited.

17. DISTRIBUTION STATEMENT (of the abstract entered in Block 20, if different from Report)

18. SUPPLEMENTARY NOTES

Available in DDC

19. KEY WORDS (Continue on reverse side if necessary and identify by block number)

calibrating	porosity (test section)	angles (flow)
aerodynamic	force balance	
wind tunnel	flow	
Mach number	probes	

20. ABSTRACT (Continue on reverse side if necessary and identify by block number)

A wedge wing on a force balance, designed for use at Mach numbers 1.6 and 2.0, has been evaluated as a continuously moving flow angle probe and calibrated in the range of Mach numbers from 0.6 to 1.3 in the AEDC Aerodynamic Wind Tunnel (4T). Moving at standard speeds of the Captive Trajectory System (CTS), it proved to be accurate and highly repeatable when operating in the three translational modes and the roll mode. It was less accurate in the

20. ABSTRACT (Continued)

pitch and yaw motions. An extensive survey made at Mach number 0.6 shows the flow direction in the 4T to be upward and toward the north wall with maximum components of 0.58 deg in pitch and 0.52 deg in yaw.

PREFACE

The work reported herein was conducted by the Arnold Engineering Development Center (AEDC), Air Force Systems Command (AFSC), Arnold Air Force Station, Tennessee. The results were obtained by ARO, Inc. (a subsidiary of Sverdrup & Parcel and Associates, Inc.), contract operator of AEDC, AFSC, under Program Element 64719F. The work was done under ARO Project No. PA412, and the manuscript (ARO Control No. ARO-PWT-TR-74-88) was submitted for publication on September 25, 1974.

CONTENTS

		Page
1.0	INTRODUCTION	7
2.0	APPARATUS	
	2.1 Wind Tunnel	7
	2.2 Support System	8
	2.3 Test Article	8
	2.4 Instrumentation	9
3.0	TEST OBJECTIVES	9
4.0	PROCEDURE	
	4.1 Test Conditions	10
	4.2 Test Procedure	10
	4.3 Data Reduction	10
	4.4 Precision of Measurement	11
	4.5 Data Acquisition Rates	11
5.0	RESULTS	
	5.1 Probe Calibrations	12
	5.2 Flow Angle Measurements	12
6.0	CONCLUSIONS	15
	REFERENCES	16

ILLUSTRATIONS

Figure		
1.	Tunnel 4T Test Section, CTS, and Region Surveyed	17
2.	Captive Trajectory System with Flow Angle Probe	18
3.	Flow Angle Probe	19
4.	Flow Angle Probe Geometry	20
5.	Functional Block Diagram of the Computer-Controlled CTS Operation and Data Processing	21
6.	Schematic of Flow Angle Probe Calibration	22
7.	Typical Calibrations Based on Normal Force	
	a. $M = 0.6$	23
	b. $M = 1.3$	24
8.	Confidence Limits on Random Errors in the Calibration Data	25
9.	Sensitivity of the Probe to Flow Angle	26

Figure | Page

10. Flow Angle Measured in the Pitch Plane on Longitudinal Traverses at M = 0.6
    a. Y = 12, Z = -12 27
    b. Y = 12, Z = 0 28
    c. Y = 12, Z = 12 29
    d. Y = 0, Z = -12 30
    e. Y = 0, Z = 0 31
    f. Y = -12, Z = -12 32
    g. Y = -12, Z = 0 33
    h. Y = -12, Z = 12 34
11. Flow Angle Measured in the Yaw Plane on Longitudinal Traverses at M = 0.6
    a. Y = 12, Z = -12 35
    b. Y = 12, Z = 0 36
    c. Y = 12, Z = 12 37
    d. Y = 0, Z = -12 38
    e. Y = 0, Z = 0 39
    f. Y = 0, Z = 12 40
    g. Y = -12, Z = -12 41
    h. Y = -12, Z = 0 42
    i. Y = -12, Z = 12 43
12. Flow Angle Measured on the Centerline Longitudinal Traverses at M = 1.3
    a. Pitch Plane 44
    b. Yaw Plane 45
13. Effect of Direction of Probe Travel on Flow Angle Measurement Based on Pitching Moment
    a. Pitch Plane Component, Y Axis 46
    b. Pitch Plane Component, Z Axis 47
    c. Yaw Plane Component, Z Axis 48
14. Flow Angle in the Pitch Plane at X = 0, M = 0.8
    a. Six Inches below the Centerline 49
    b. Nine Inches below the Centerline 50
    c. Twelve Inches below the Centerline 51
15. Flow Angle in the Yaw Plane at X = 0, M = 0.8
    a. Three Inches below the Centerline 52
    b. Six Inches below the Centerline 53

Figure Page

15. Continued
    c. Nine Inches below the Centerline 54
    d. Twelve Inches below the Centerline 55
16. Comparison of Data Obtained at Same Point during Different Probe Motions at M = 0.6
    a. Normal-Force Data 56
    b. Pitching-Moment Data 57
17. Data Obtained during Probe Rolls on the Centerline 58
18. Direct Indication of True Flow Angle Compared with Vector Sum of the Components at M = 0.6 59

TABLES

1. Results of the Aerodynamic Calibrations of the Probe 60
2. Probe Travel and Data Scan Information 61
3. Coefficients of the Least-Squares Line Fits to the Probe Aerodynamic Calibration Data 62
4. Confidence Limits on Random Errors in Calibration Data 63

APPENDIX

A. DATA REDUCTION EQUATIONS 64

NOMENCLATURE 66

1.0 INTRODUCTION

The plans for calibration of the Mach number 1.6 and 2.0 nozzle blocks in the Aerodynamic Wind Tunnel (4T) of the Propulsion Wind Tunnel Facility (PWT) included three phases: (1) determination of tunnel operating parameters by measuring static pressures along a pipe at the test section centerline, (2) assessment of Mach number uniformity by surveying a region in the test section with a pitot rake attached to the Captive Trajectory System (CTS), and (3) measurement of flow angles in the same region with a probe attached to the CTS. Only Phase 1 could be completed in the time available, and its results were presented in Ref. 1. In addition to obtaining the test section flow angle data in phase 3, an evaluation of a wedge on a balance as a flow angle probe was planned. It was believed that a probe having sensitivity to flow direction in terms of a somewhat extended area might be superior for use in a partially open-wall tunnel to one with sensitivity in terms of two very localized pressures. Although it was the characteristics of supersonic flow which led to this conclusion, and even though the wedge design was based on considerations of flow at Mach number 1.6 and above, it seemed likely that such a probe could be useful throughout the range of Mach numbers available for testing in PWT. Therefore, an entry in Tunnel 4T was planned for calibration and evaluation of the probe in the subsonic and transonic Mach number range.

The standard procedure for acquiring data in Tunnel 4T has involved movement of a sensing instrument or a model into position, followed by a pause for instrument scan, data reduction, and printout for each data point. This, of course, is necessary for pressure data from other than very closely coupled transducers. However, with more sophisticated instrumentation having come into use in PWT in recent years, it seemed appropriate to investigate the possibility of making measurements, with a balance, at a series of locations with the probe in continuous motion. The project plan thus evolved into the following: (1) development of a data acquisition procedure, (2) programming for maximum automatic operation and minimum probe idle-time, (3) calibration and evaluation of the probe over the range of Mach numbers available in Tunnel 4T with only the sonic nozzle, and (4) determination of the feasibility and applicability of reading continuously changing balance data, with existing PWT instrumentation and equipment, while moving in each of the six CTS degrees of freedom.

2.0 APPARATUS

2.1 WIND TUNNEL

Tunnel 4T is a closed-loop continuous-flow tunnel capable of developing Mach numbers from 0.1 to 1.3 using the sonic nozzle, and 1.6 and 2.0 using appropriately contoured overlays. The stagnation pressure range is from 160 to 3400 psfa. The test section (see Fig. 1) is 4 ft square by 12.5 ft long with porous walls that can be set to vary the open area from near zero to 10 percent. Suction through the porous walls is used to maximize flow uniformity and to develop supersonic flow with the sonic nozzle. The wall hole pattern can be seen in Figs. 2 and 3, and a more detailed description of the tunnel is given in Ref. 1.

2.2 SUPPORT SYSTEM

The CTS (pictured in Fig. 2) was used to support the flow angle probe. It is an electromechanical system with six degrees of freedom and all axes of motion are contained within a single mechanism that is independent of the main sting system. The d-c electric drive motors can bring the sting up to the following maximum velocities in 0.1 sec:

Movement	Maximum Velocity
Longitudinal	1.7 in./sec
Transverse	5.2 in./sec
Vertical	1.3 in./sec
Pitch	10.4 deg/sec
Yaw	10.4 deg/sec
Roll	55.0 deg/sec

The positioning envelope of the CTS pitch center extends to Y and Z = ±15 in. from the tunnel centerline and X = ±18 in. from a reference pitch center located at tunnel station 133.25. Pitch and yaw motions are obtained to a maximum of ±45 deg and the sting can be rolled ±360 deg.

The CTS can be operated manually with controls located adjacent to the tunnel. It can be controlled automatically by the Raytheon 520 digital computer from punched card input instructions or by a Xerox Data Systems (XDS) CF16 Mini-Computer operating on commands from the Raytheon 520.

For any axis, the overall positioning error is normally maintained at less than 0.2 percent of full-scale travel. However. the repeatability of the data obtained during this test indicates that the positioning errors in pitch and yaw, significant parameters in this test, were considerably less than 0.2 percent of full scale.

A complete description of the CTS is given in Ref. 2.

2.3 TEST ARTICLE

The wedge-balance assembly pictured in Figs. 2 and 3 was designed specially as a probe for measuring flow angles in Tunnel 4T at Mach numbers 1.6 and 2.0. The wedge (see Fig. 4) was sized for use on the CTS with safe loading up to total pressures of 2000 psfa and angles of attack of ±2 deg. The balance is a two-component, normal-force and pitching-moment unit with the gage sections made as thin as was feasible to give maximum sensitivity. It was protected from failure by sizing the probe sleeve into which the balance fits so that it will foul on the balance body before the stresses in the gage sections become excessive. The balance was gaged using standard materials and procedures.

2.4 INSTRUMENTATION

Tunnel 4T shares portions of the data acquisition system of the PWT 16-ft Supersonic Wind Tunnel (16S). It is an automatic data recording system with one of two Raytheon 520 computers as the heart of the system. In addition, an XDS CF16 Mini-Computer performs scan, data acquisition, and control functions for Tunnel 4T. In this test, it controlled the positioning of the CTS, normally done by the Raytheon 520, and its 8192-word memory and high internal speeds made it possible to obtain data with continuous travel of the probe. Force measurements were recorded by a computer-controlled digital data acquisition system with a capacity of 28 channels and a range of 10 mv to 10 v. A functional block diagram of the computer-controller operation of the CTS and data processing is presented in Fig. 5.

3.0 TEST OBJECTIVES

The primary objective of the test was to establish the capability of a small wing on a balance as a flow angle probe from the standpoints of credibility, accuracy, and reliability. Measurement of small angles, generally less than one-half degree, is required for evaluation of wind tunnel flow quality. In supersonic flow within a porous wall test section, the disturbance pattern can impose pressure differences between the opposite orifices of a flow angle probe which are a significant percentage of the pressure difference representative of the mean flow angle. A probe having sensitivity to flow direction in terms of a somewhat extended area should be superior for use in a partially open-wall tunnel to one with sensitivity in terms of two very localized pressures. So that the probe could be fully evaluated, plans were made to calibrate it in both subsonic and supersonic flow. It was also desired to establish the pattern of variation of flow direction throughout the principal test region of 4T for at least one Mach number, as an indication of what further measurements might be beneficial.

An important secondary objective which developed after initiation of test planning was to show the feasibility of obtaining force and moment data during continuous model movement with existing PWT instrumentation. Finally, it was desirable to establish the feasibility of programming for automatic control of the CTS and scanning of the probe data throughout the test region in a "hand off" operation to minimize the idle-time of the probe and to minimize test time.

4.0 PROCEDURE

4.1 TEST CONDITIONS

Probe calibrations were obtained at Mach numbers 0.6, 0.8, 0.9, 1.0, 1.1, and 1.3. The stagnation pressure was set between 1100 and 2000 psfa, as listed in Table 1, the stagnation temperature varied from 80 to 105°F, and the specific humidity ranged from 0.0026 to 0.013.

4.2 TEST PROCEDURE

After the tunnel conditions were established, two distinct sets of procedures were followed, one for calibration of the probe, the other for flow angle measurement.

For probe calibration, several operational steps were ordered manually, bringing the probe into position on the tunnel centerline at Station 108 and setting up all instrumentation for proper operation. The next order initiated automatic CTS operation, data acquisition, and data printout. The automatic CTS operation was not the standard operation by the Raytheon 520 computer from punched card input, but instead, pitching and rolling instructions were written into the data reduction program and acted upon by the CF16 Mini-Computer to obtain nine data points each in the upright and inverted positions, with the probe leading edge held in a fixed location. The probe was at rest during scans of calibration data.

Flow angle measurements were made during continuous probe movements in the directions of the X, Y, and Z axes, during pitch and yaw motions, and through 360 deg rolls (see Fig. 1). Control of the CTS was still by the CF16 Mini-Computer but from punched card input. The CF16 scanned and retained the data until the end of an excursion or roll, whereupon the data were transmitted to the Raytheon 520 computer, reduced, and the results printed, in a one-point-at-a-time stepping procedure (see Fig. 5). The sequence of data scans for one probe excursion or roll consisted of a specified number of points, taken at a fixed time interval while the probe was in motion, and one point taken with the probe at rest at the end of the movement.

4.3 DATA REDUCTION

The standard 4T program for calculation and printout of tunnel conditions, geometry, etc., was used to reduce the data from permanent instrumentation. Standard balance equations were used to reduce the force and moment data. The data reduction equations as specialized for this test are given in Appendix A.

The program was written to obtain two independent calibrations, in terms of normal force and of pitching moment, and to calculate flow angles from each calibration. Straight-line, least-squares fits of the probe calibration data were calculated by the Raytheon 520, from which it determined the sensitivity to flow direction and a correction for asymmetry of the probe, as well as the flow angle in the pitch plane at the probe location. Figure 6 schematically illustrates the derivation of these quantities from the data. The necessary calibration data were retained in the Raytheon 520 for calculation of flow angles.

4.4 PRECISION OF MEASUREMENT

The flow angularity measurements of this test are those with respect to the tunnel centerline, which is a level line midway between opposite sidewalls of the test section. The test model was leveled on the CTS rig in pitch and roll using a bubble level with an accuracy of better than 0.01 deg. The zero yaw angle was set by measuring the distance of fore and aft points on the model from the side walls and equalizing the distances. This produced an uncertainty in the zero yaw angle of about 0.01 deg also. Therefore, the minimum uncertainty in the flow angle measurements is ±0.01 deg. However, examination of the model calibration data and of repeated points shows a linearity, resolution, and repeatability smaller than 0.01 deg in many cases. The precision of measurement of the flow angles by the wedge probe is discussed in Section 5.1, Probe Calibrations. The precision of measurement of the other variables of this test are as follows for a 95-percent confidence level:

Mach number:	$2\sigma(M)$ =	±0.002
Total pressure:	$2\sigma(p_t)$ =	±2 psfa
CTS coordinates:	$2\sigma(X)$ =	±0.036 in.
	$2\sigma(Y)$ =	±0.030 in.
	$2\sigma(Z)$ =	±0.030 in.
	$2\sigma(\nu)$ =	±0.090 deg
	$2\sigma(\eta)$ =	±0.090 deg
	$2\sigma(\omega)$ =	±0.72 deg

4.5 DATA ACQUISITION RATES

Standard CTS speeds were used during this test because the objective was to evaluate the usefulness of the probe and procedures under standard conditions rather than to evaluate the limiting speeds for acquisition of acceptable data. The probe speeds and extent of movement, the time interval for data scans, and the number of data points specified for an excursion or roll are listed in Table 2. The speeds listed are those calculated from the performance during this test.

5.0 RESULTS

5.1 PROBE CALIBRATIONS

Calibrations to determine sensitivity of the probe to flow direction and to evaluate the effect of probe asymmetry were obtained in terms of both normal force and pitching moment. Plots of normal force calibration data at Mach numbers 0.6 and 1.3 are shown in Fig. 7. These plots are typical; all other plots evidence the same degree of linearity and negligible scatter. Calibration line-fit coefficients are listed in Table 3, and the parameters derived from these fits are listed in Table 1. At the only Mach number at which stagnation pressure was varied, M = 0.6, the sensitivity to flow angle is lower and the local flow angle is greater at the higher p_t. The indications of probe asymmetry, $C_{N,o}$ and $C_{m,o}$, Table 1, if converted to angular asymmetry, show the probe to be of nearly perfect symmetry.

The quality of the least-squares fits of the calibration data is revealed by the standard deviations, $\sigma(C_N)$ and $\sigma(C_m)$, which are presented in Table 4 after conversion to 2σ values. Also included in this table are 2σ deviations in the equivalent flow angle, $2\sigma(\theta_{C_N})$ and $2\sigma(\theta_{C_m})$, which are the coefficient 2σ deviations divided by the coefficient slopes. These 2σ deviations for the equivalent flow angle are representative of the precision of measurement of the flow angle and are plotted in Fig. 8. On the basis of this figure, it is assumed that the precision in setting the probe's pitch angle is about 0.02 deg or less over the ±2-deg angle range used in this test. This is evident from the $2\sigma(\theta)$ values that were obtained at Mach number 1.3. The smallest value on the figure is applicable because the CTS rig has no cognizance of what Mach number flow is present in the test section; hence, there should be no Mach number effect on the performance of this mechanism. The calibrations based on normal force and on pitching moment are of equal accuracy. The statistical data derived from the probe calibrations and shown in Fig. 8 are considered as representative of the precision to be expected of the flow angle measurements.

The sensitivities to flow angle are shown in Fig. 9. It is clear that better definition of sensitivity in the supersonic range would be desirable.

5.2 FLOW ANGLE MEASUREMENTS

5.2.1 Traverse Data

Longitudinal traverses were made at M = 0.6 at all tunnel cross-sectional points where both Y and Z are equal to ±12 or 0 (see Fig. 1) and at M = 1.3 on the centerline. At X = 0, excursions were made laterally at Z = 0 and vertically at Y = 0, at M = 0.6, and laterally at Z = -12, -9, -6, and -3 at M = 0.8.

The measurements in the pitch plane made on longitudinal traverses at M = 0.6 are shown in Fig. 10. The measurements based on pitching moment and on normal force are in agreement except for two traverses (Figs. 10b and h) where consistent small differences are shown. There is little variation with tunnel station except at Y = Z = 12 (Fig. 10c). Similar measurements in the yaw plane are shown in Fig. 11. Differences between the measurements by force and by moment are generally small as are variations with tunnel station. Data obtained from longitudinal traverses at M = 1.3 are shown in Fig. 12, where axial variation of flow angle in both the pitch and the yaw plane is much in evidence.

It is now clear that, just as with the calibration data, the flow angle measurements based on normal force and on pitching moment are of equal accuracy. Therefore, only the pitching-moment measurements during traverses on the Y and the Z axes at M = 0.6 are shown in Fig. 13 so that the effect of direction of probe motion can be clearly seen. The complete traverses on the Y axis (Fig. 13a) show a variation of flow angle with Y which should allow easy detection of an effect of direction of travel, yet the data taken with the probe moving in opposite directions fall on the same curve. Data were acquired during only a portion of the traverses on the Z axis (Figs. 13b and c), but there is enough overlap to show that all the data fall on one curve.

A portion of this same transverse plane at Tunnel Station 108 (X = 0) was traversed in the Y direction at M = 0.8. The measurements in the pitch plane are shown in Fig. 14. There is little difference between the lateral distributions at 12, 9, and 6 in. below the centerline, all showing considerable variation with Y. The measurements in the yaw plane are shown in Fig. 15, where less similarity in the lateral distribution is seen, and the variation with Y is shown to be greater nearer the centerline.

Measurements made at Mach numbers 0.6, 0.8, and 1.3, almost without exception, show the flow to be upward and toward the right looking upstream. The maximum measurements in an opposite direction were 0.1 deg. The maximum vertical flow angle values were 0.58, 0.35, and 0.20 deg at Mach numbers 0.6, 0.8, and 1.3, respectively. The maximum horizontal flow angle values were 0.52, 0.56, and 0.30 deg at M = 0.6, 0.8, and 1.3, respectively. These flow angles are acceptably low according to the general criteria of Ref. 3.

5.2.2 Evaluation of the Probe and the Data Acquisition Procedure

Some evaluation data were discussed in Section 5.2.1 and shown in Fig. 13, where traverses in opposite directions show no effect attributable to time lag of the probe reaction or of any instrumentation. The comparison between the two traverses in each section of the figure also shows excellent repeatability. In Figs. 10 through 15, the data taken after the probe came to rest, shown usually as multiple points on one edge of the plot, show almost no deviation from the curves of the data taken during motion.

There are nine points in the region surveyed at Mach number 0.6 where data were obtained during as many as four of the following types of probe motion: traverses on X, Y, and Z and rolls of 360 deg. These data are grouped for illustration of their agreement at the individual points in Fig. 16. The highest rms values of the deviations from the arithmetic mean at a point are 0.023 deg for the yaw plane flow angle measured by normal force at X = Y = 0 and Z = 12, and 0.022 deg for the pitch plane flow angle measured by normal force at X = 0, Y = -12, and Z = 0.

The flow angles in the pitch and yaw planes are almost constant on the centerline at M = 0.6 (see Figs. 10e and 11e). In agreement with this fact, the five 360-deg rolls made on the centerline between X = 16 and X = -16 show almost identical curves. The envelope of all five pitching-moment flow angle curves is shown with the plotted data of X = 0 (Fig. 17), and it is seen to be very narrow.

The maximum flow angle indications from roll data obtained at X = 0, plotted at the roll angles at which they were registered, are compared in Fig. 18 with the vector sum of pitch plane and yaw plane components measured during traverses in the direction of the X, Y, and Z axes. These are all pitching-moment data, and circles of radii equal to the confidence limits from the moment calibration applicable to the data, M = 0.60 in Table 1, are also shown. These circles enclose all paired points, and circles of radii = σ would include most points.

The data discussed and displayed thus far clearly show that a small wing mounted on a balance affords a superior procedure for measuring flow direction in a wind tunnel. Measurement in terms of either normal force or pitching moment can yield flow direction data with an absolute accuracy that is but little different from the accuracy with which the probe is aligned. These data also show that reliable measurements can be made at a very rapid rate during two modes of continuous probe movement, that is, linear traverses and rolling motion. The maximum speeds at which the probe can be moved to acquire good data are higher than the standard rates of travel in the X, Y, and Z directions and in roll motion.

The data reduction Eqs. (A-11) and (A-12) take into account the deviation of the probe from parallelism with the centerline; hence, the indicated flow angle should be correct when the probe is set to angles other than $\nu = 0$ and $\eta = 0$. However, the data taken during yawing and pitching motions were not at all comparable to the data for other probe motions. Near the beginning and the end of sweeps, the computed values were quite variable. Between these portions of the sweeps, the variation was less, but the data differed from those obtained in other ways by ±0.08 deg in the pitch plane and by ±0.25 deg in the yaw plane. An accurate analysis of reasons has not been achieved, but it seems probable that the probe speeds and operational characteristics in pitch and yaw motions were principally responsible. It is believed that, at some lower speed, reliable measurements could be made.

6.0 CONCLUSIONS

Based on the results of the probe calibration and checkout, the following conclusions have been reached:

1. A small wing on a balance is an excellent instrument for measuring wind tunnel flow angularity. The mean confidence limits observed during calibration varied from ±0.05 deg at M = 0.6 to ±0.015 deg at M = 1.3. Complete traverses in the direction of the X and Y axes and portions of traverses on the Z axis show curves based on normal force and on pitching moment that are, for the most part, identical to within less than ±0.01 deg.

2. Attempts to measure flow angles during continuous movement in the direction of the X, Y, and Z axes and during continuous roll were successful. Data taken during traverses in both directions along the Y and Z axes and comparisons of data taken with the probe at rest and in motion show that the data taken during probe motion are essentially identical with data that would be measured during probe pauses. At the nine points in the field where data were obtained during two, three, or four different modes of CTS movement, the rms values of the deviations from the local arithmetic means are 0.023 deg or less at all points.

3. Attempts to take data of equal accuracy during probe sweeps at standard speed in the pitch and yaw directions were not successful, but it appeared that a lower speed may have changed this result.

4. The two-component balance produced flow angle data based on normal force and on pitching moment that are of equal quality.

5. The flow direction in 4T at M = 0.6 with only the CTS and a small probe in the tunnel is upward and toward the right looking upstream with maximum components in pitch and yaw equal to 0.58 deg and 0.52 deg, respectively. There is little longitudinal variation, but lateral and vertical variations are clearly significant.

NACA 1135

REFERENCES

1. Gunn, J. A. and Maxwell, H. "Calibration of the AEDC-PWT Aerodynamic Wind Tunnel (4T) Mach Numbers 1.6 and 2.0 Nozzle Blocks." AEDC-TR-72-111 (AD749513), September 1972.

2. Christopher, J. P. and Carleton, W. E. "Captive-Trajectory Store-Separation System of the AEDC-PWT 4-Foot Transonic Tunnel." AEDC-TR-68-200 (AD839743), September 1968.

3. Pope, A. Wind Tunnel Testing. Second Edition, John Wiley and Sons, Inc., 1954.

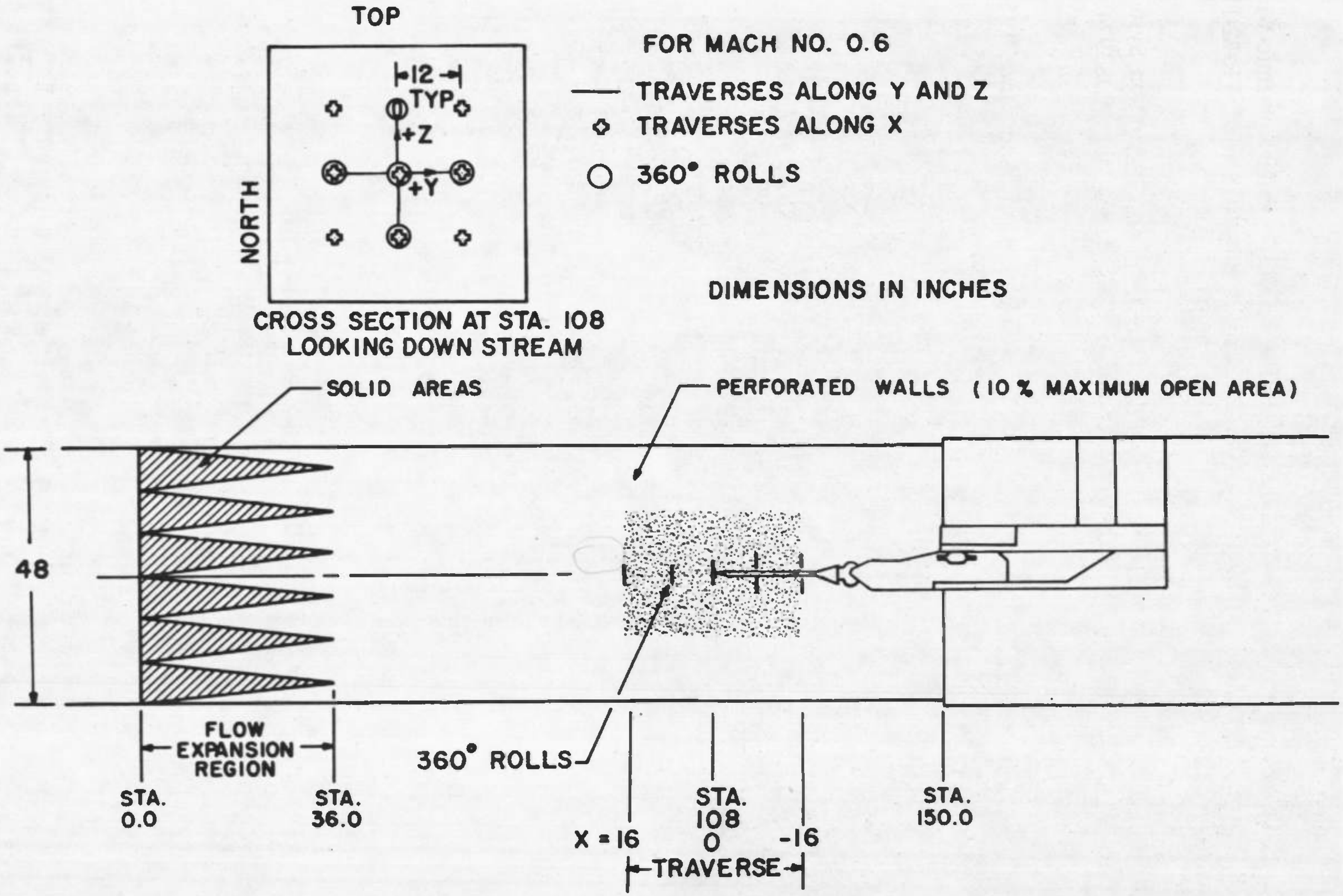

Figure 1. Tunnel 4T test section, CTS, and region surveyed.

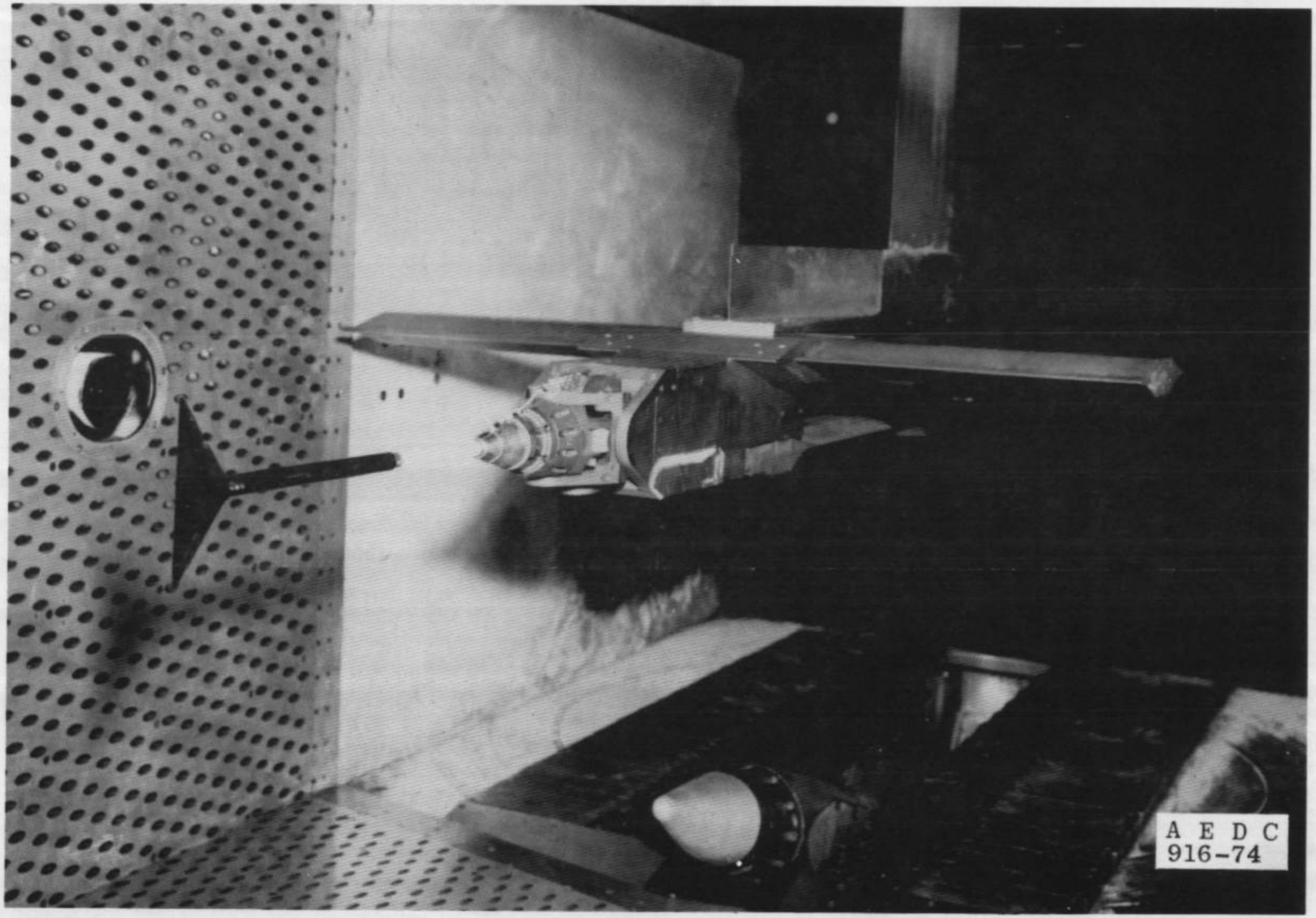

Figure 2. Captive trajectory system with flow angle probe.

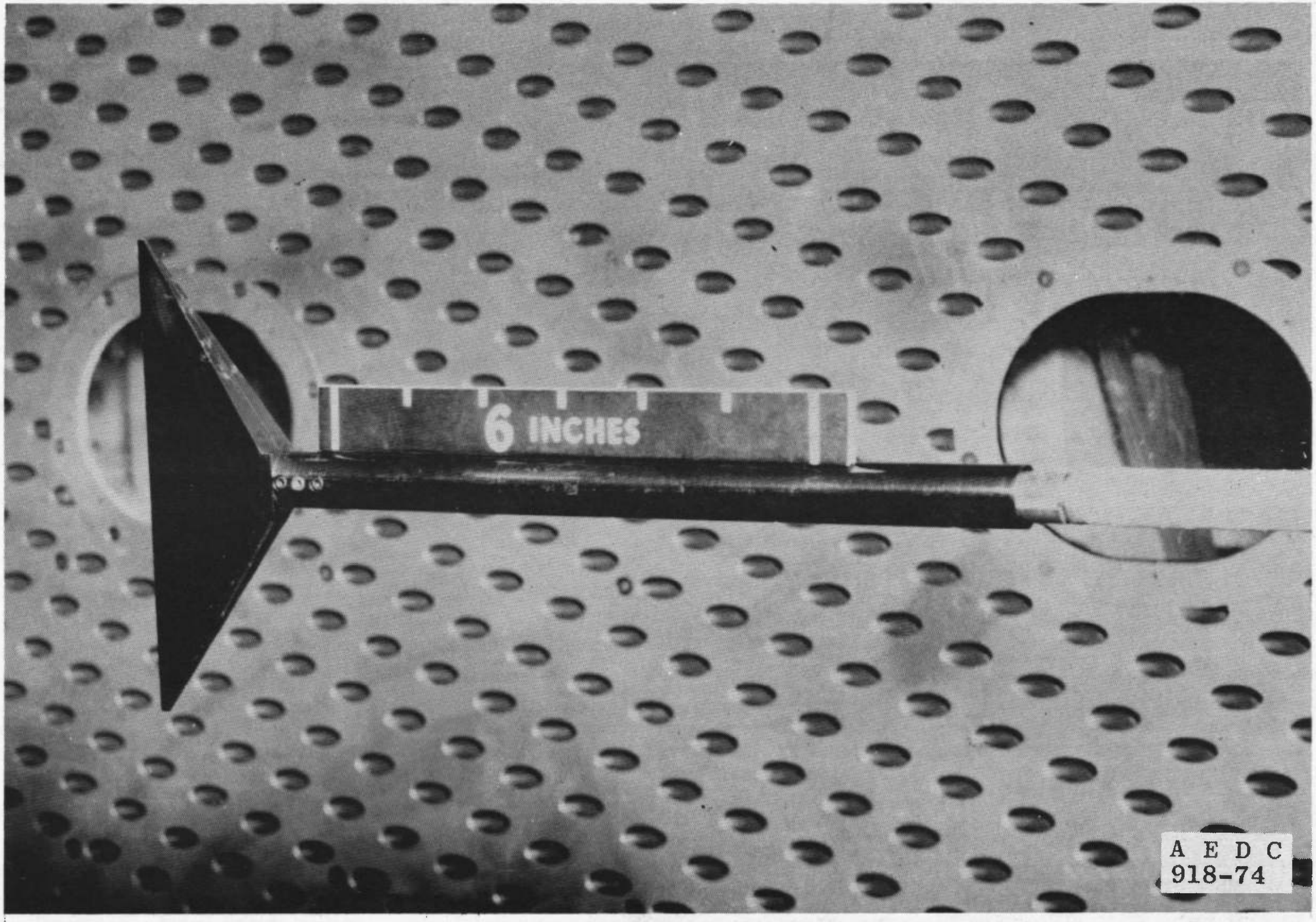

Figure 3. Flow angle probe.

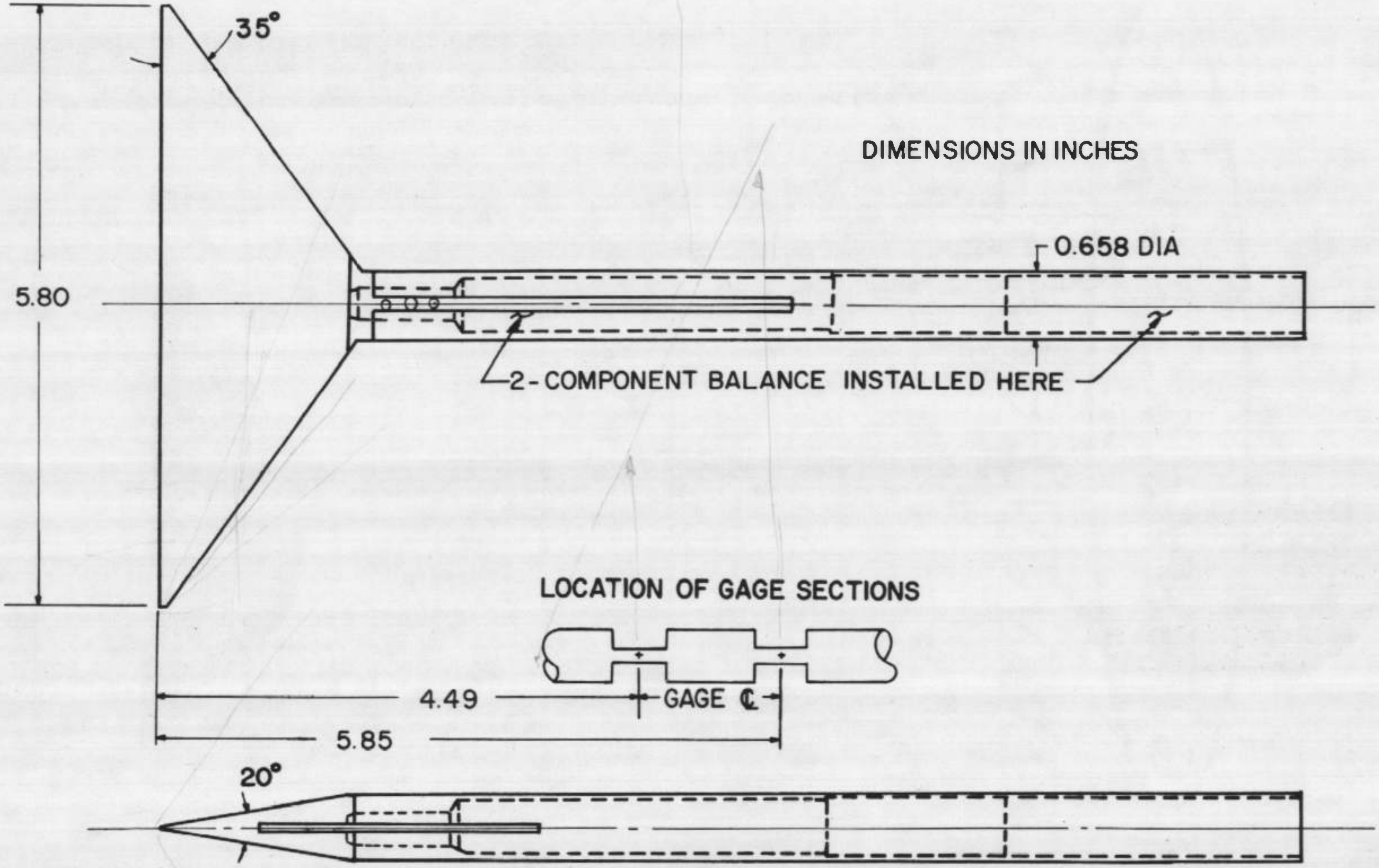

Figure 4. Flow angle probe geometry.

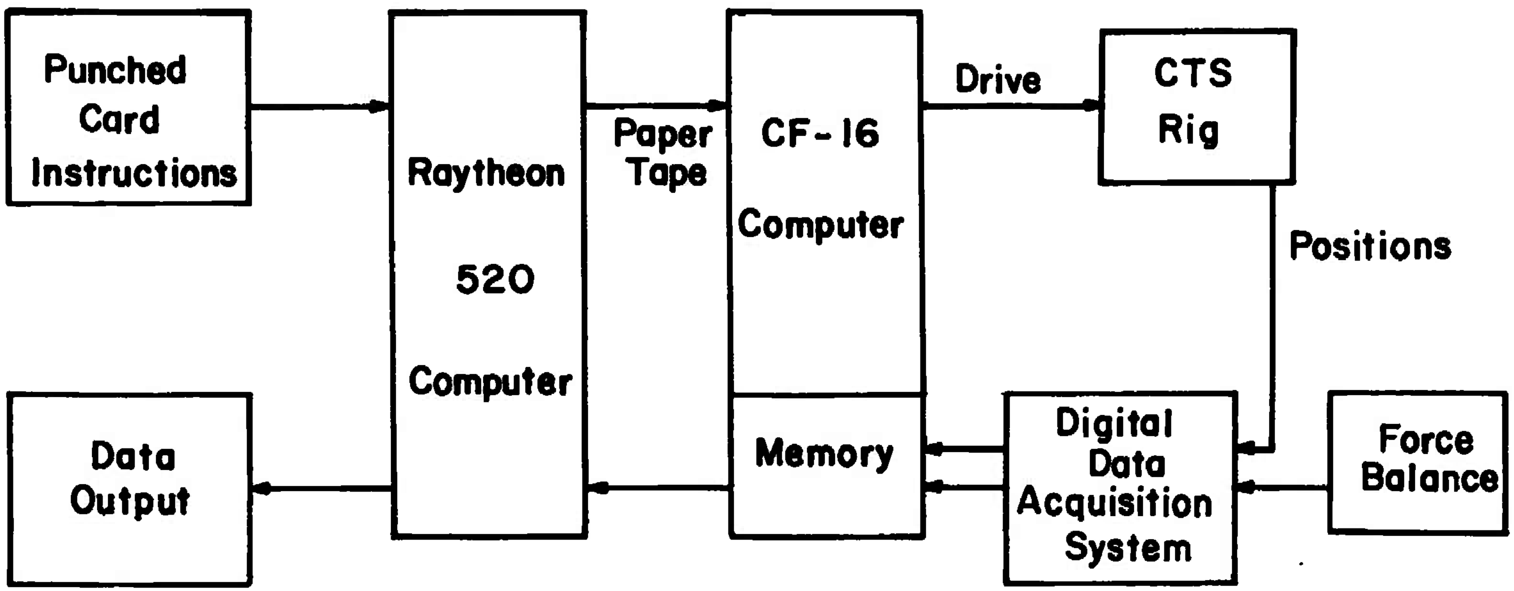

Figure 5. Functional block diagram of the computer-controlled CTS operation and data processing.

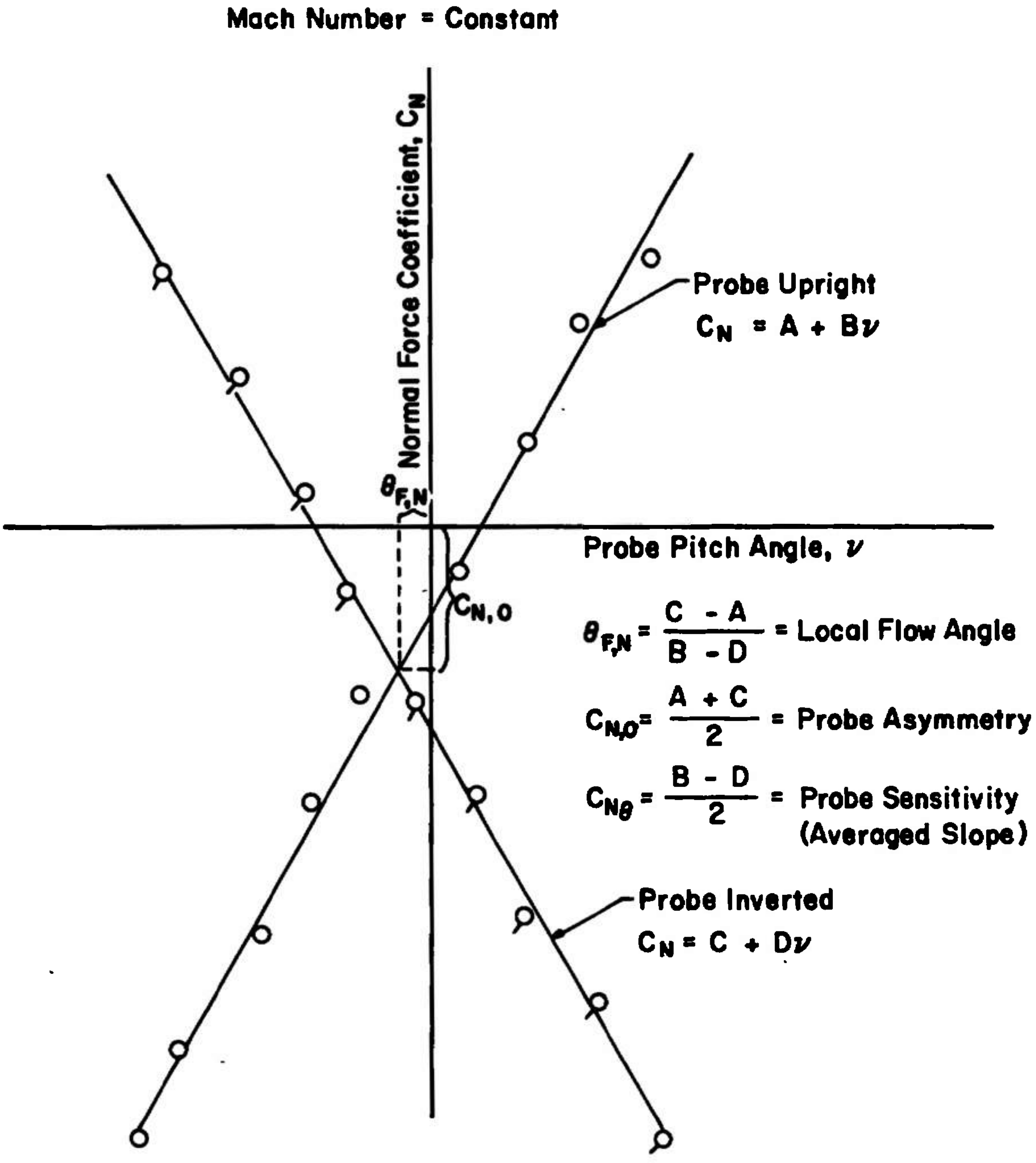

Figure 6. Schematic of flow angle probe calibration.

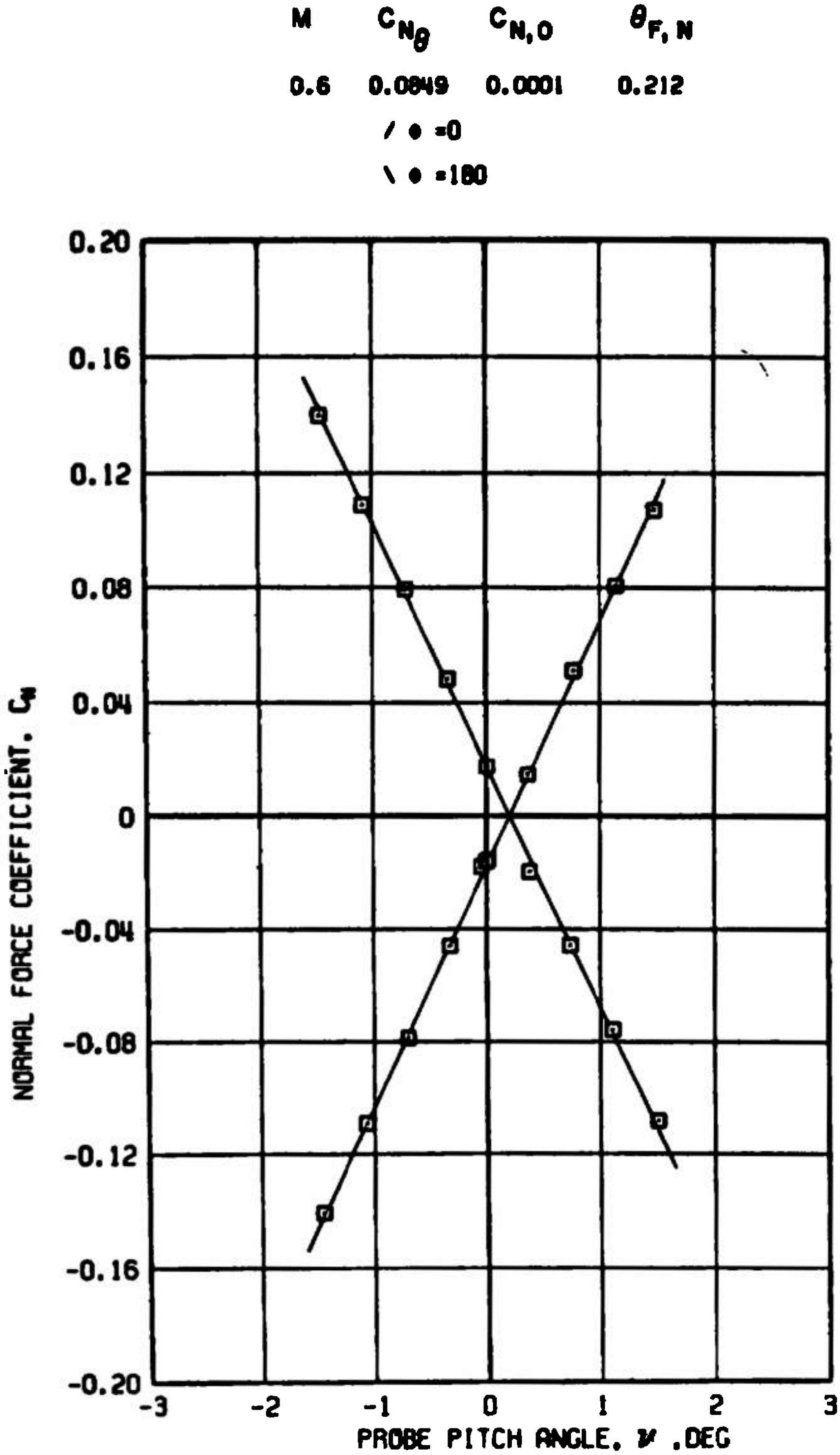

a. M = 0.6
Figure 7. Typical calibrations based on normal force.

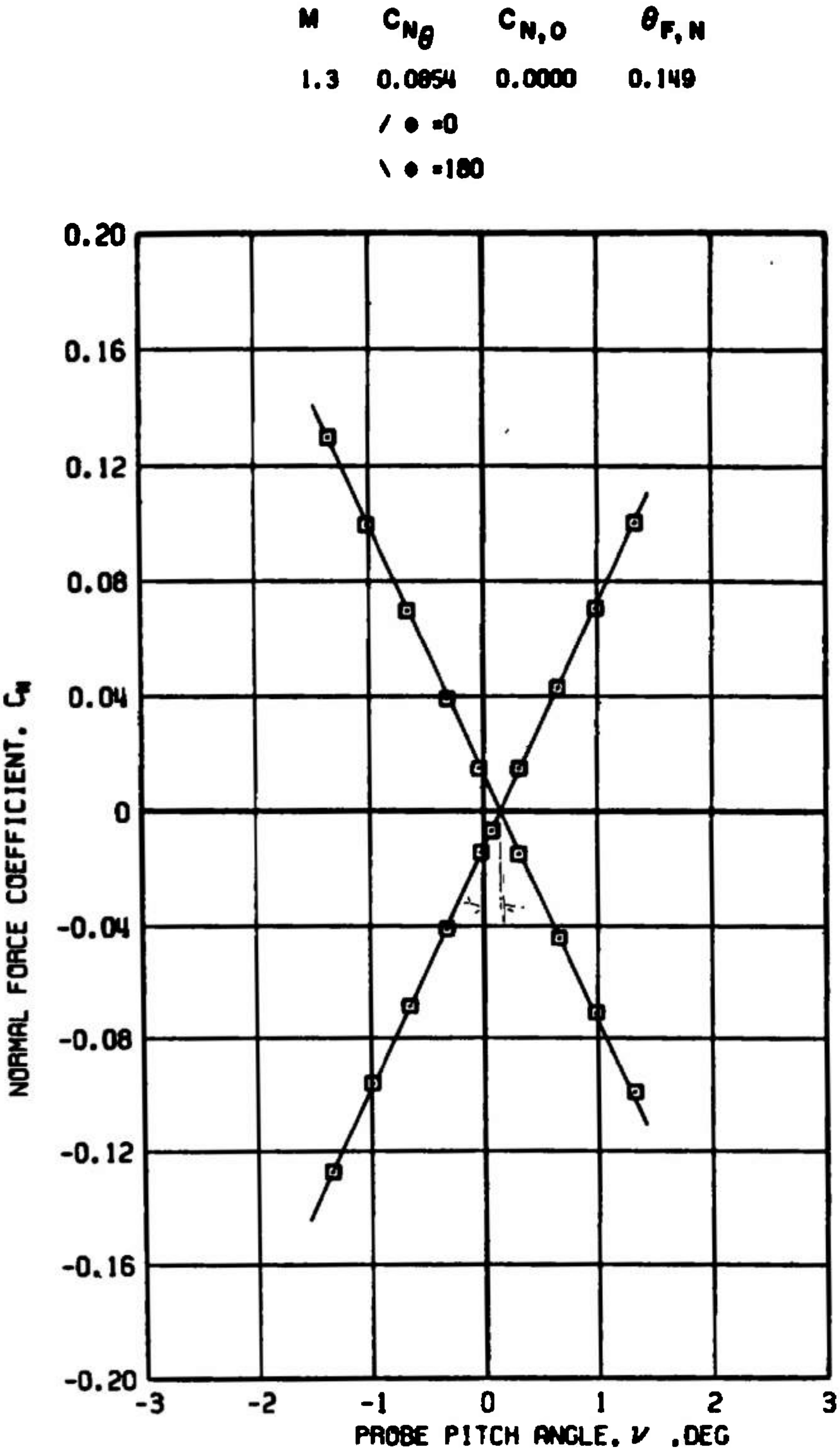

b. M = 1.3
Figure 7. Concluded.

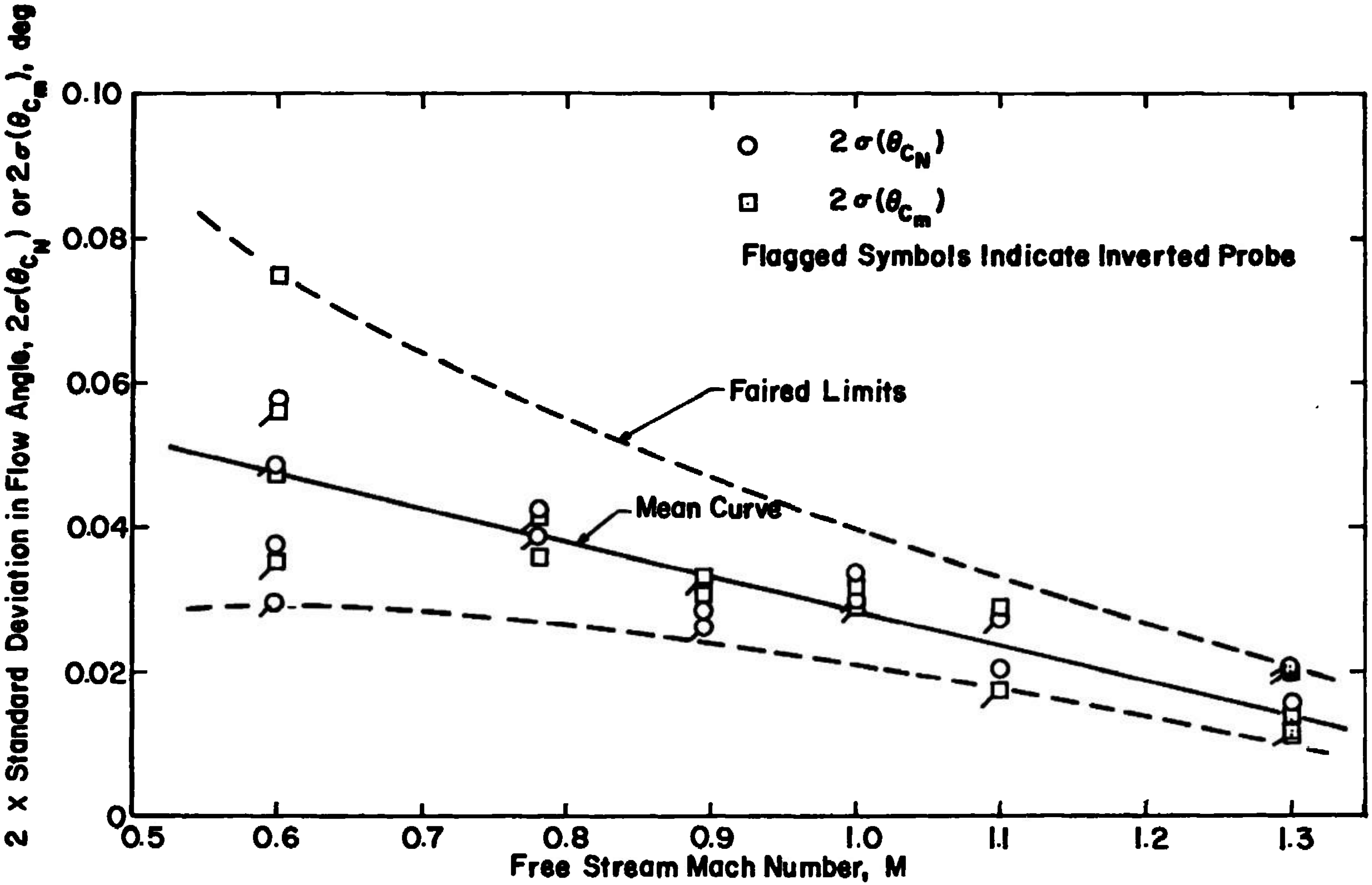

Figure 8. Confidence limits on random errors in the calibration data.

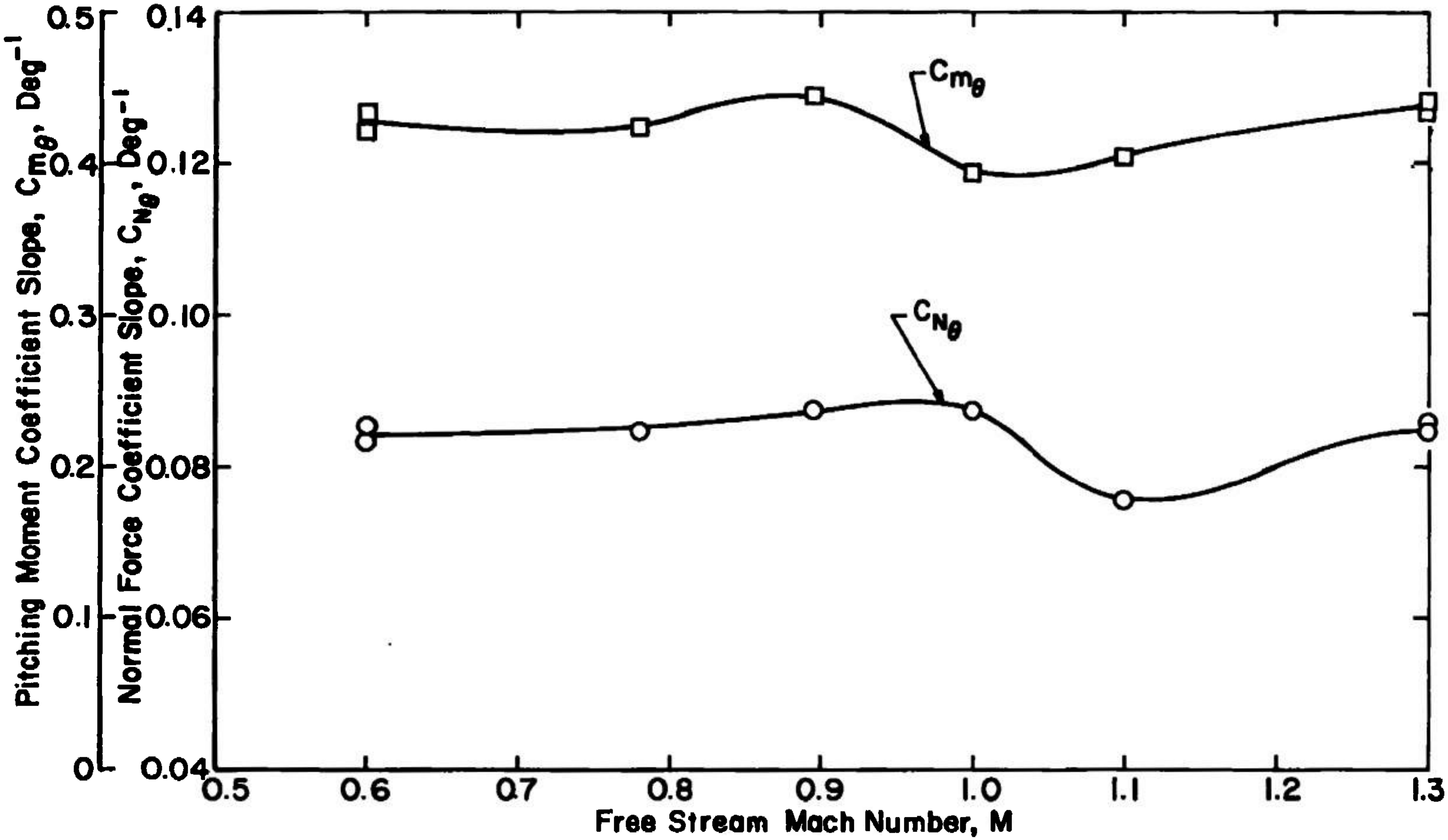

Figure 9. Sensitivity of the probe to flow angle.

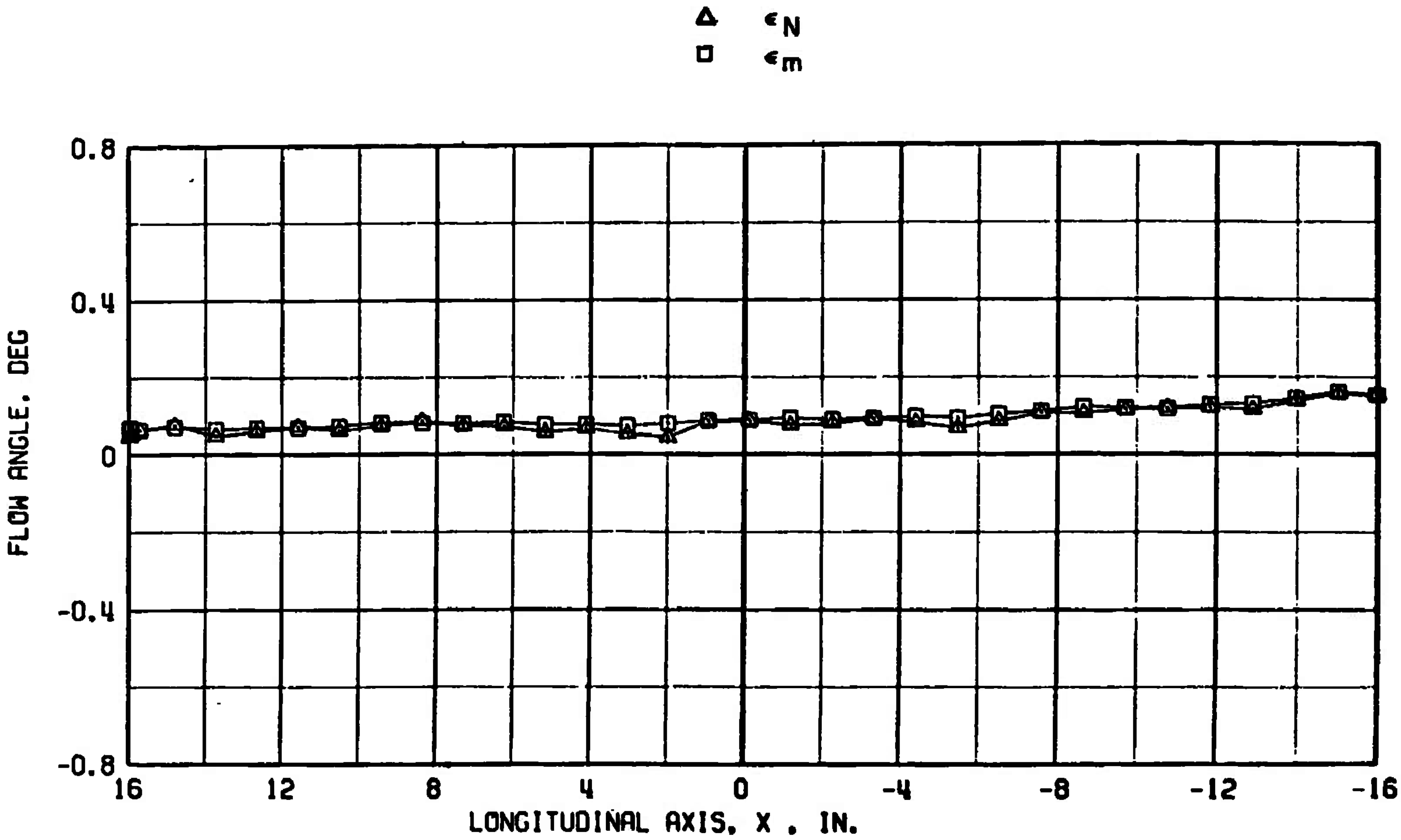

a. Y = 12, Z = -12

Figure 10. Flow angle measured in the pitch plane on longitudinal traverses at M = 0.6.

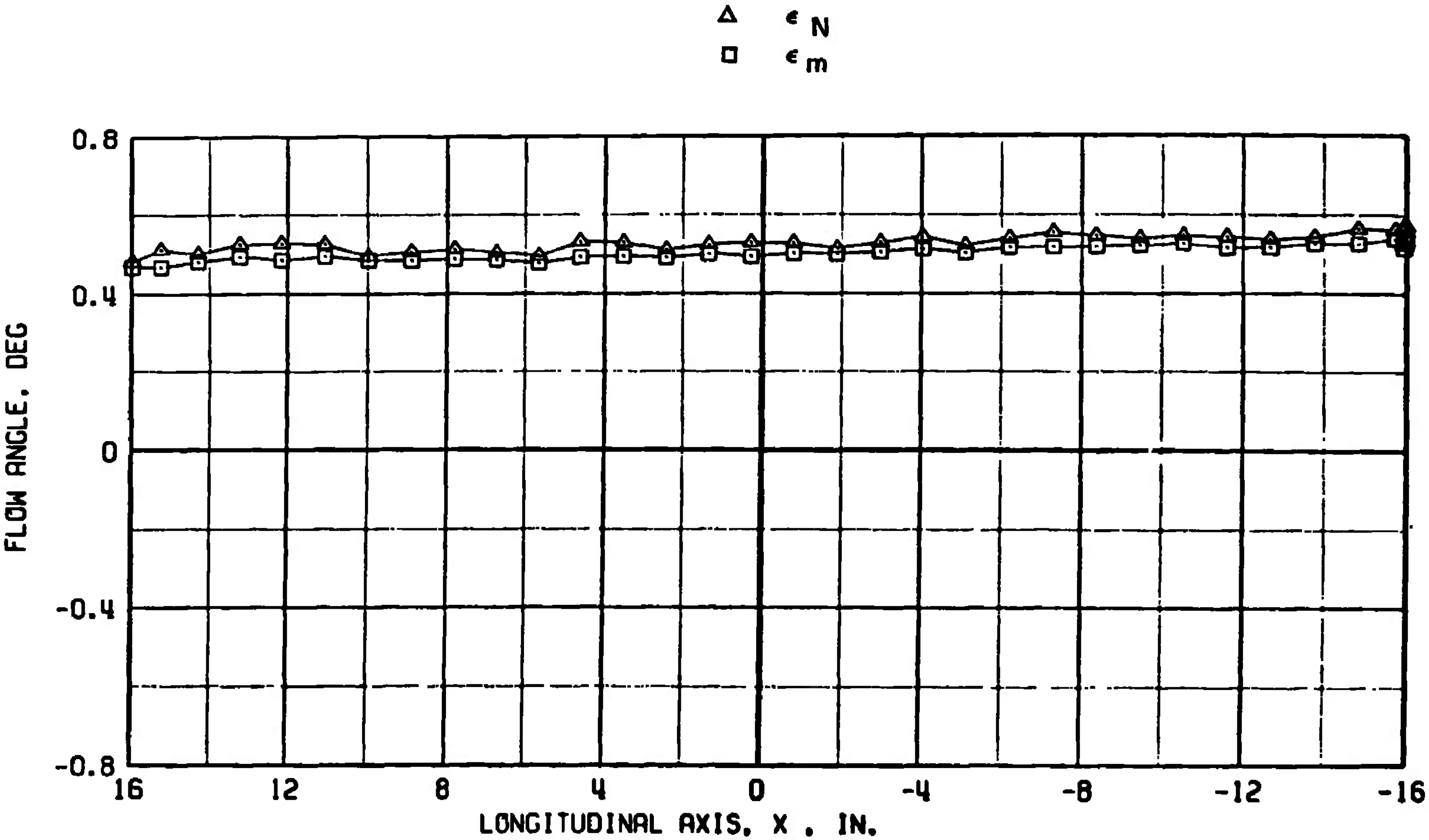

b. Y = 12, Z = 0
Figure 10. Continued.

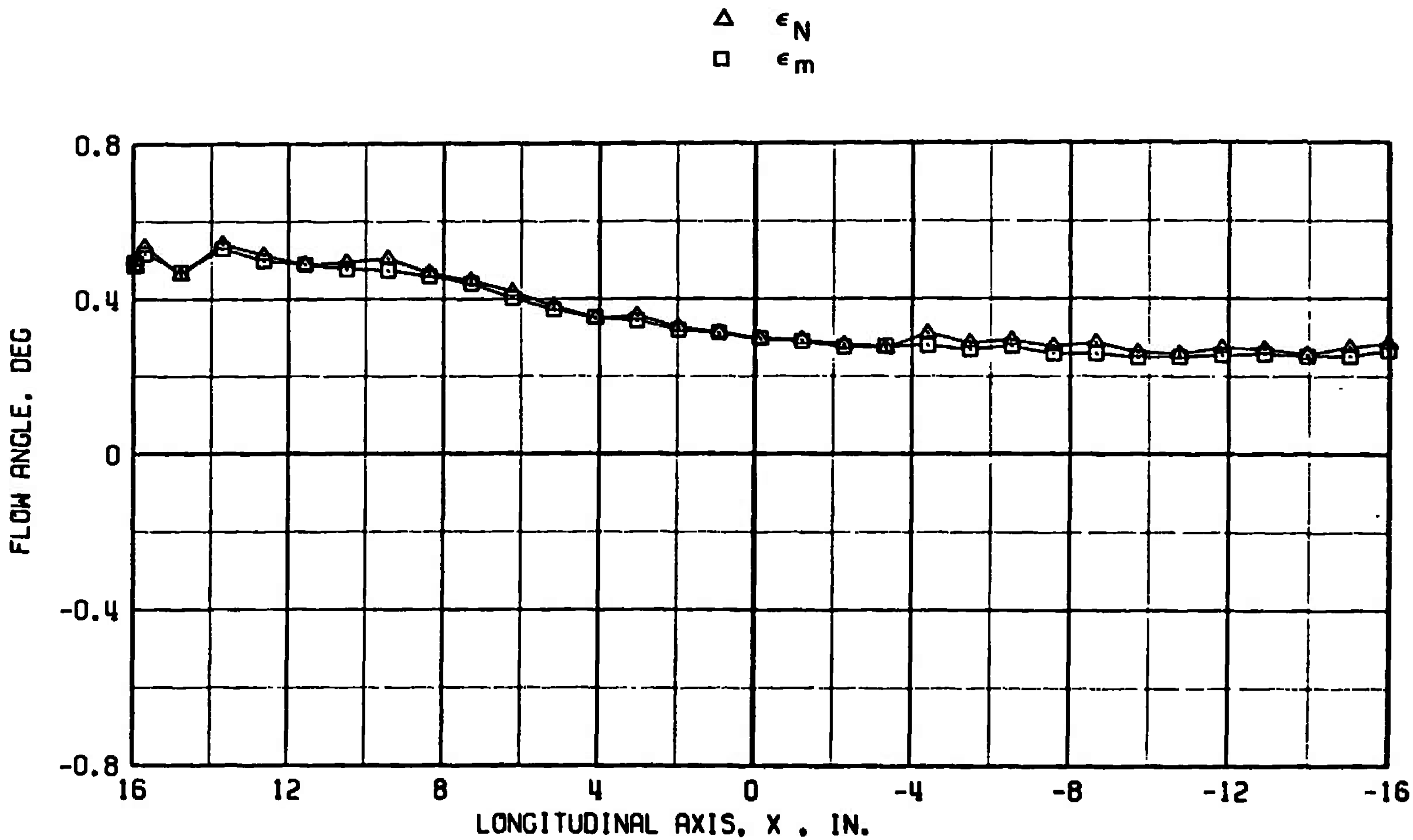

c. Y = 12, Z = 12
Figure 10. Continued.

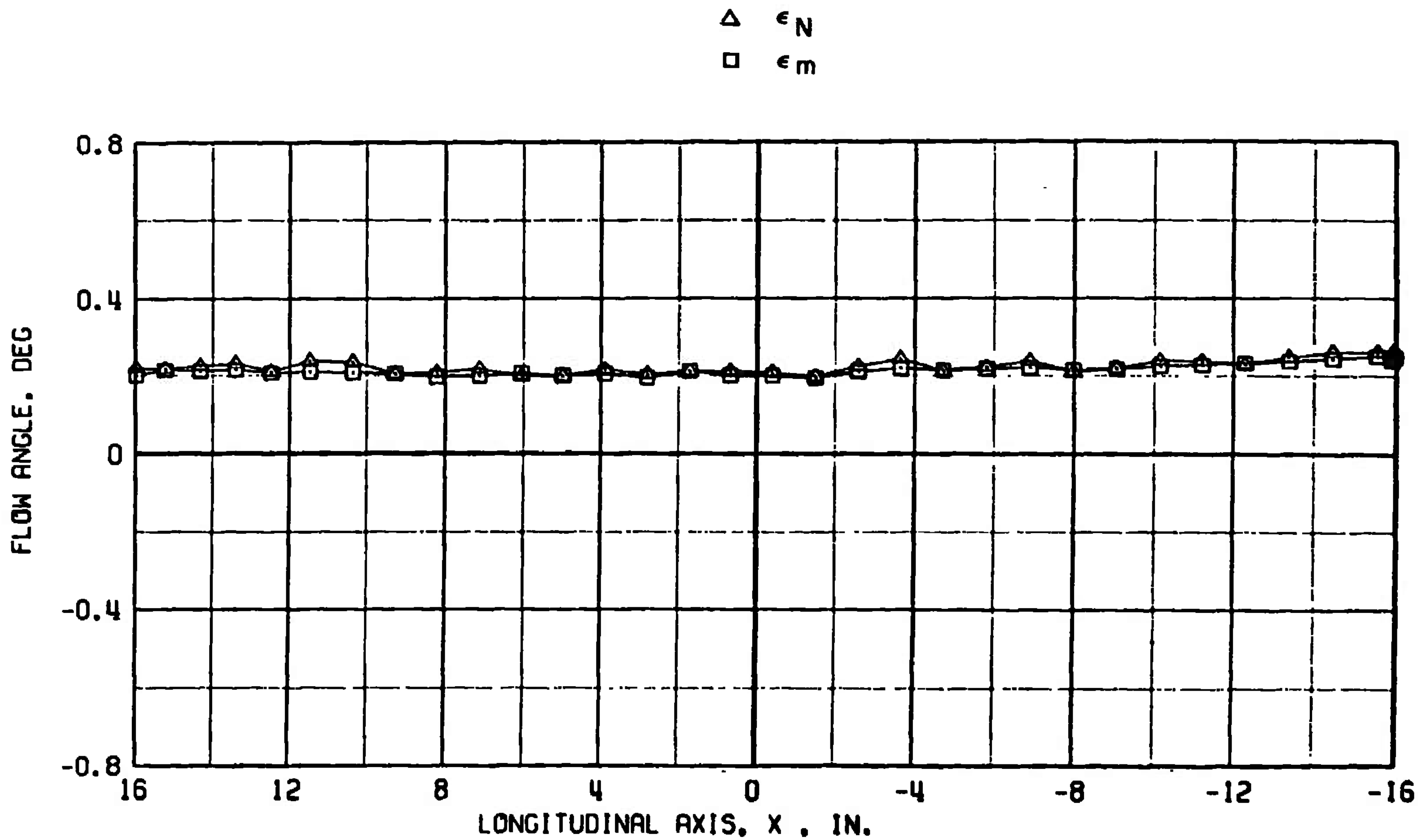

d. Y = 0, Z = -12
Figure 10. Continued.

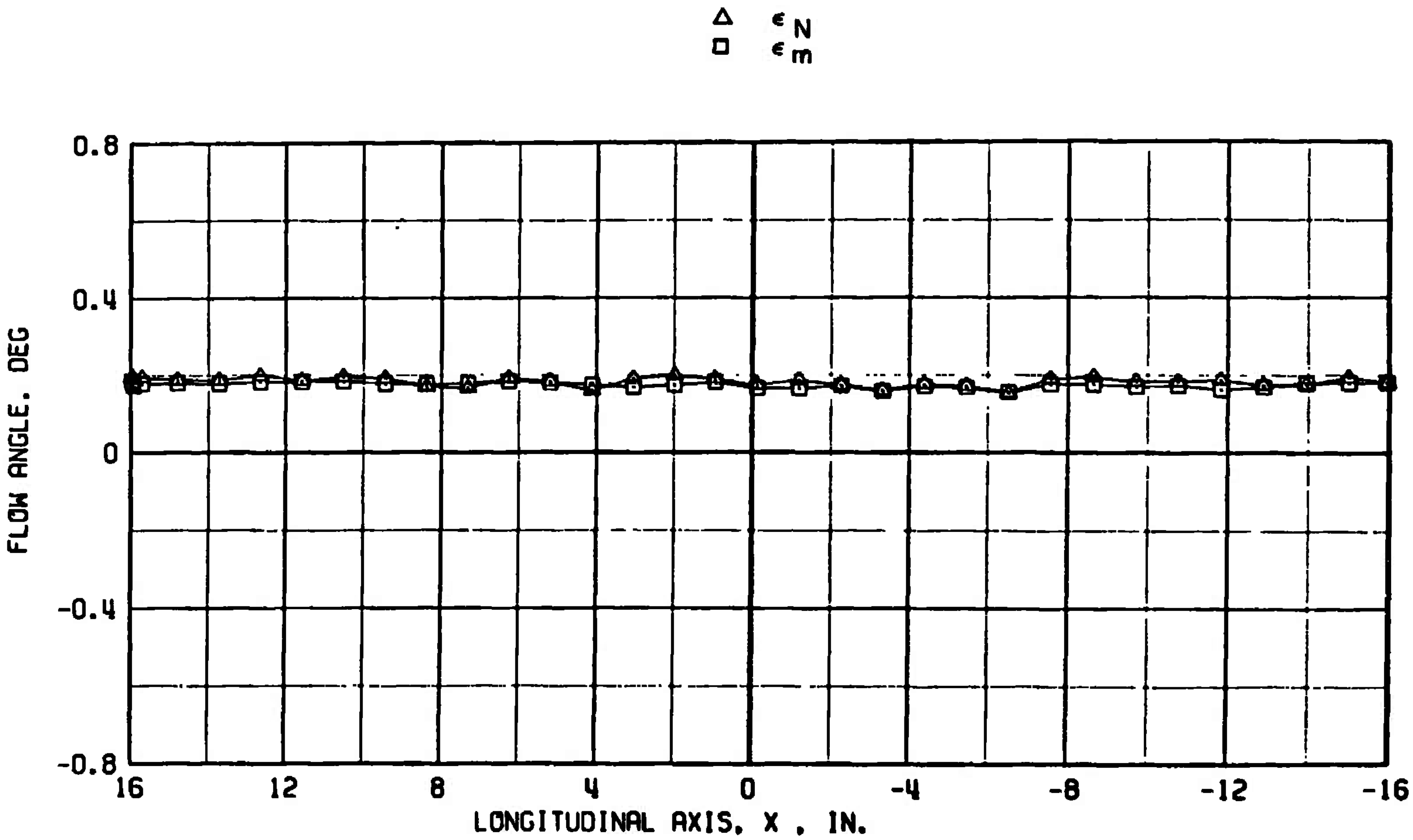

e. Y = 0, Z = 0
Figure 10. Continued.

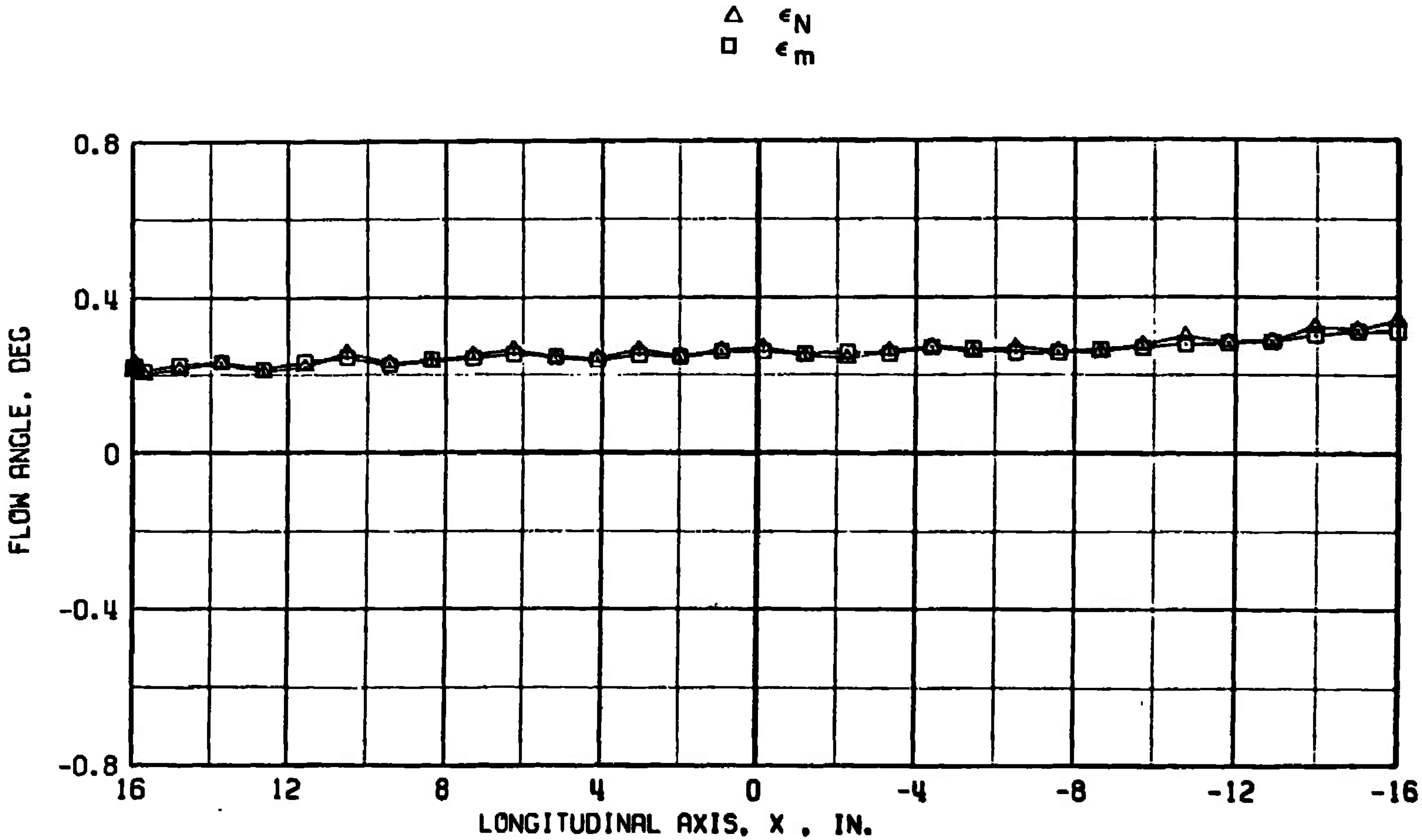

f. Y = -12, Z = -12
Figure 10. Continued.

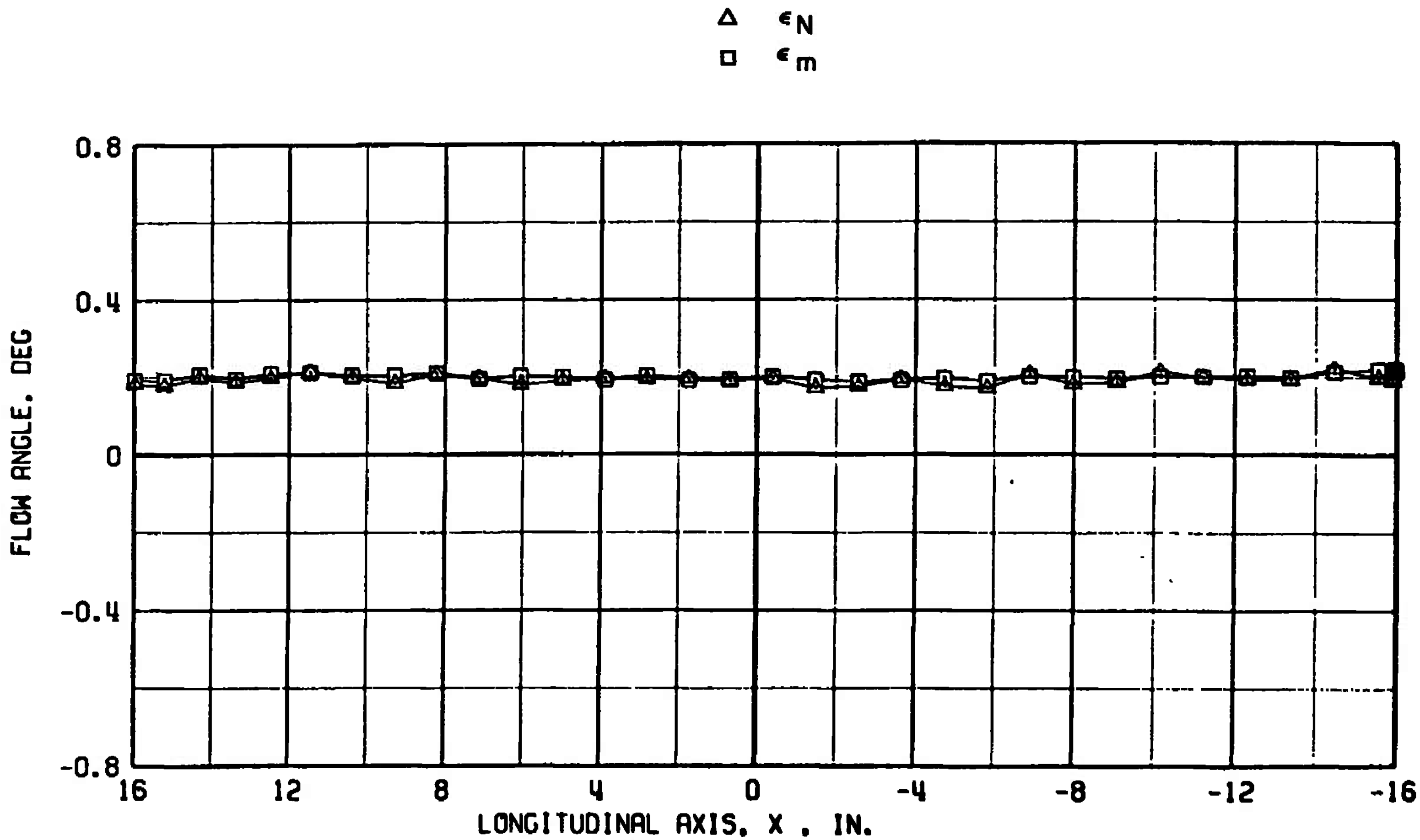

g. Y = -12, Z = 0
Figure 10. Continued.

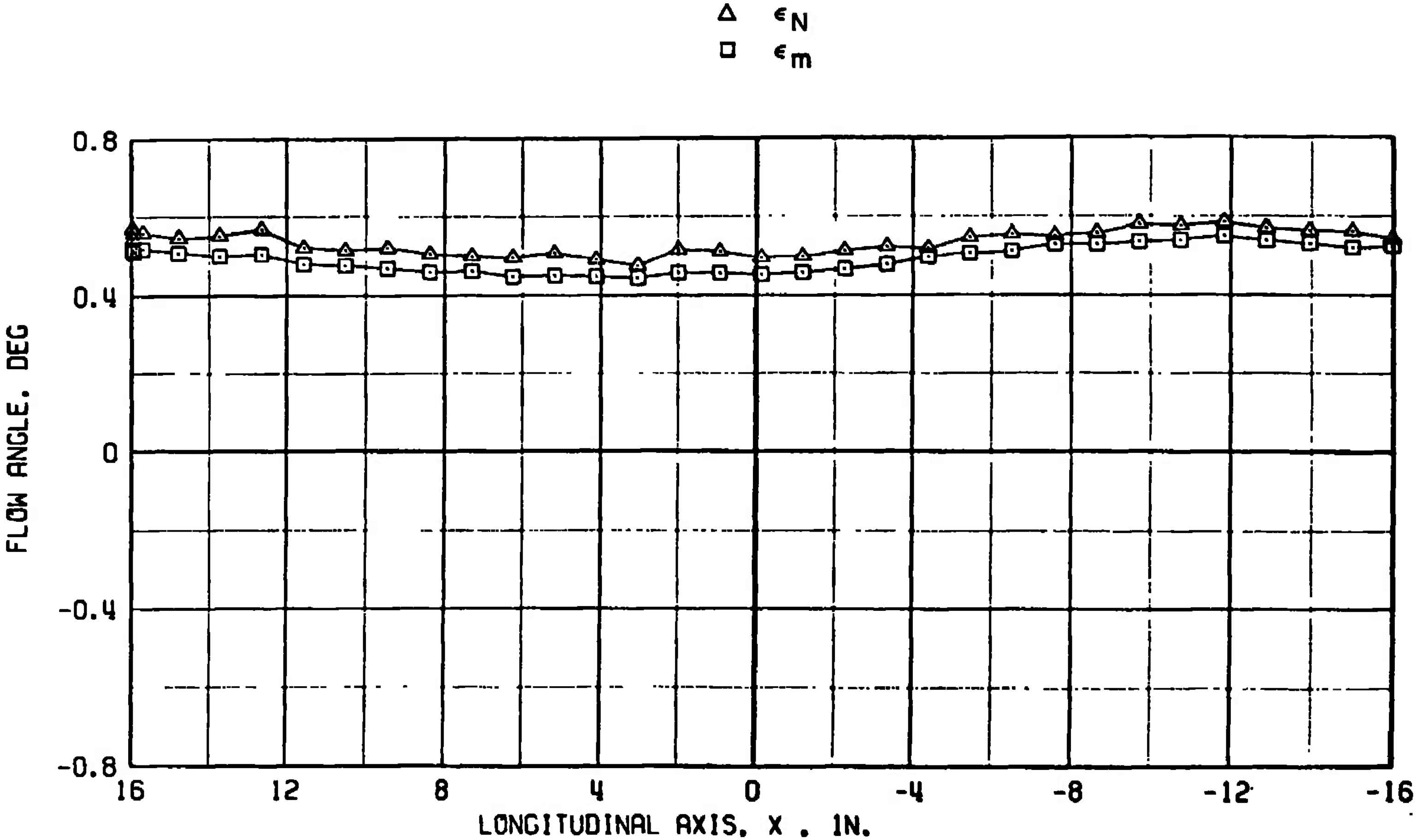

h. Y = -12, Z = 12

Figure 10. Concluded.

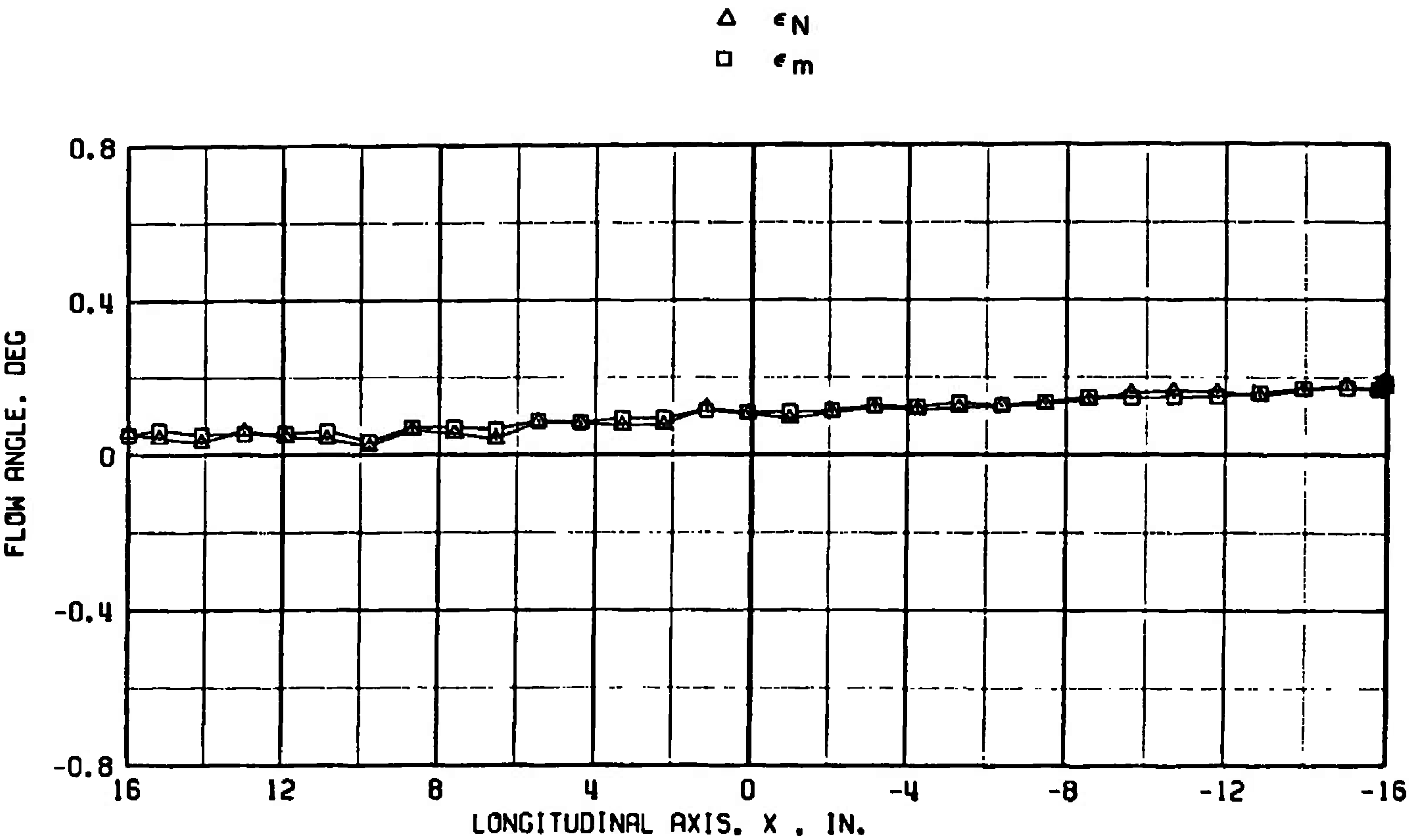

a. Y = 12, Z = -12

Figure 11. Flow angle measured in the yaw plane on longitudinal traverses at M = 0.6.

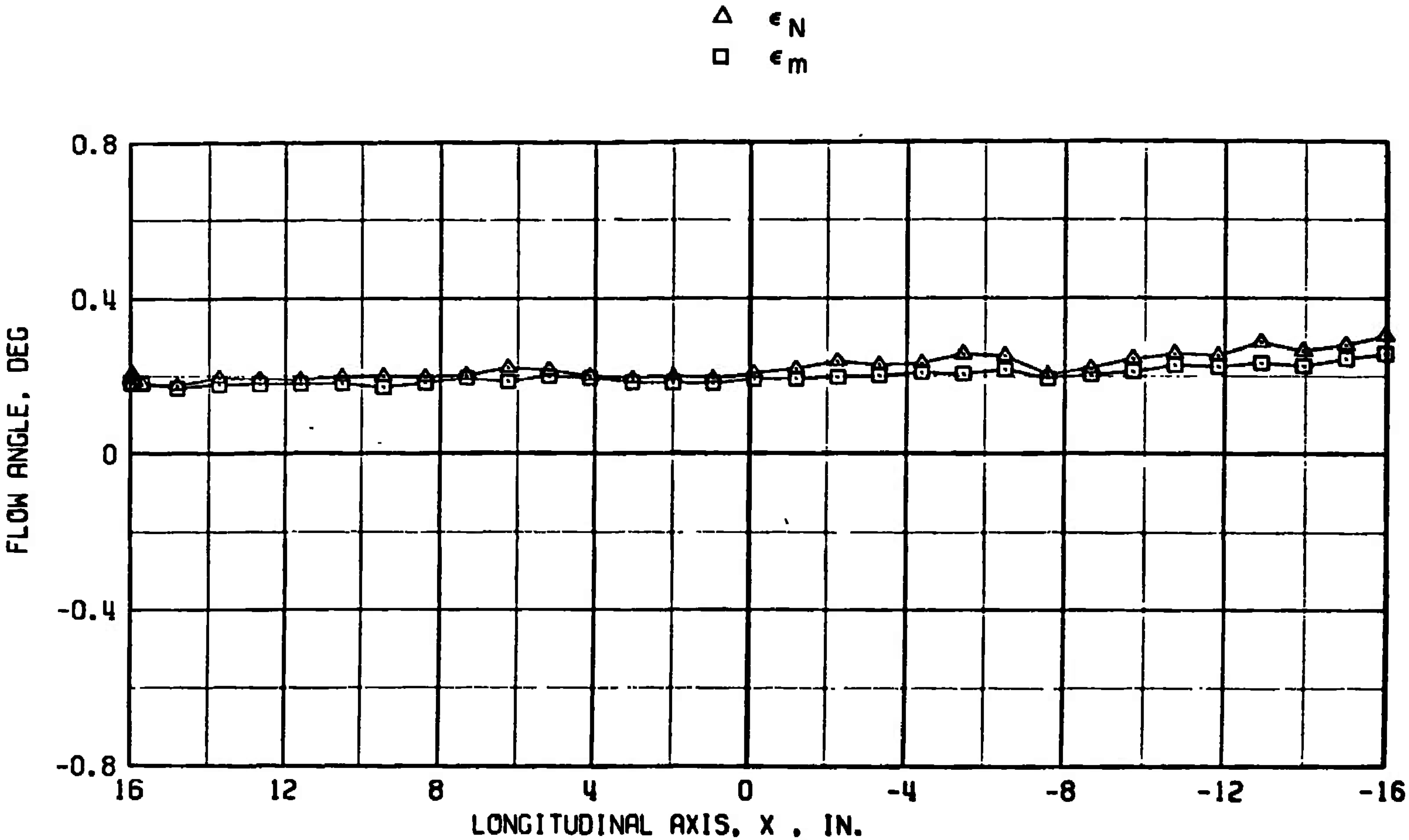

b. Y = 12, Z = 0
Figure 11. Continued.

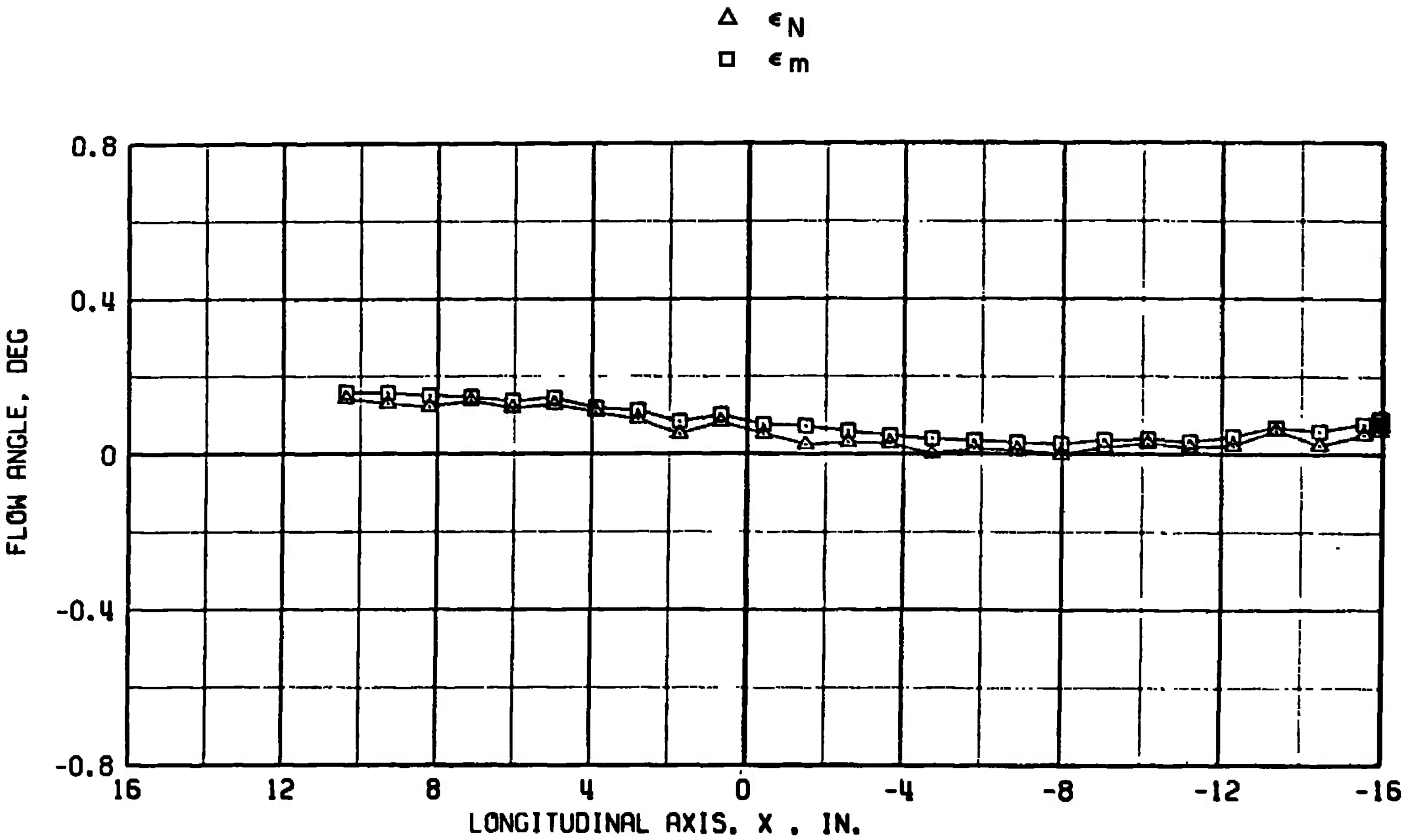

c. Y = 12, Z = 12
Figure 11. Continued.

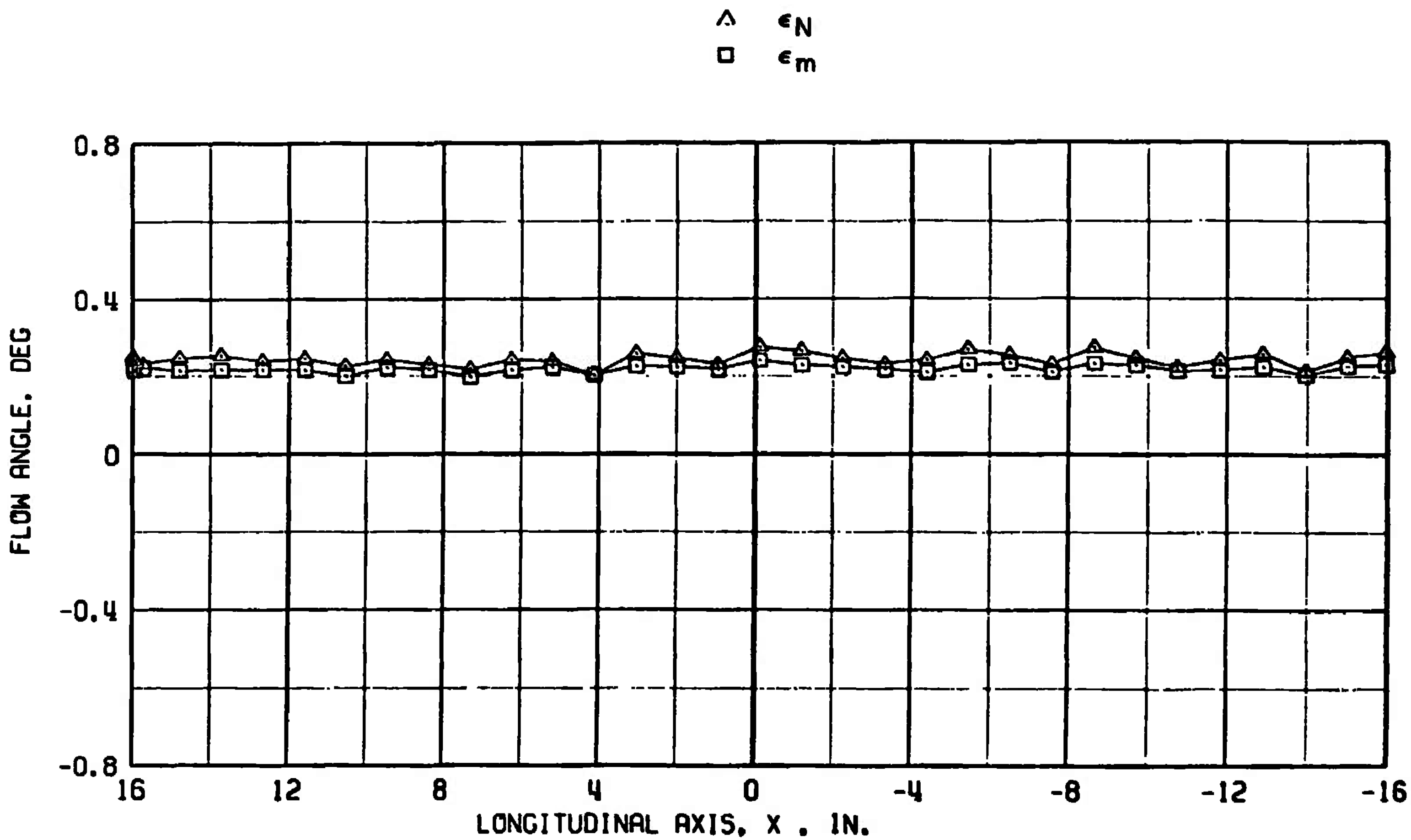

d. Y = 0, Z = -12
Figure 11. Continued.

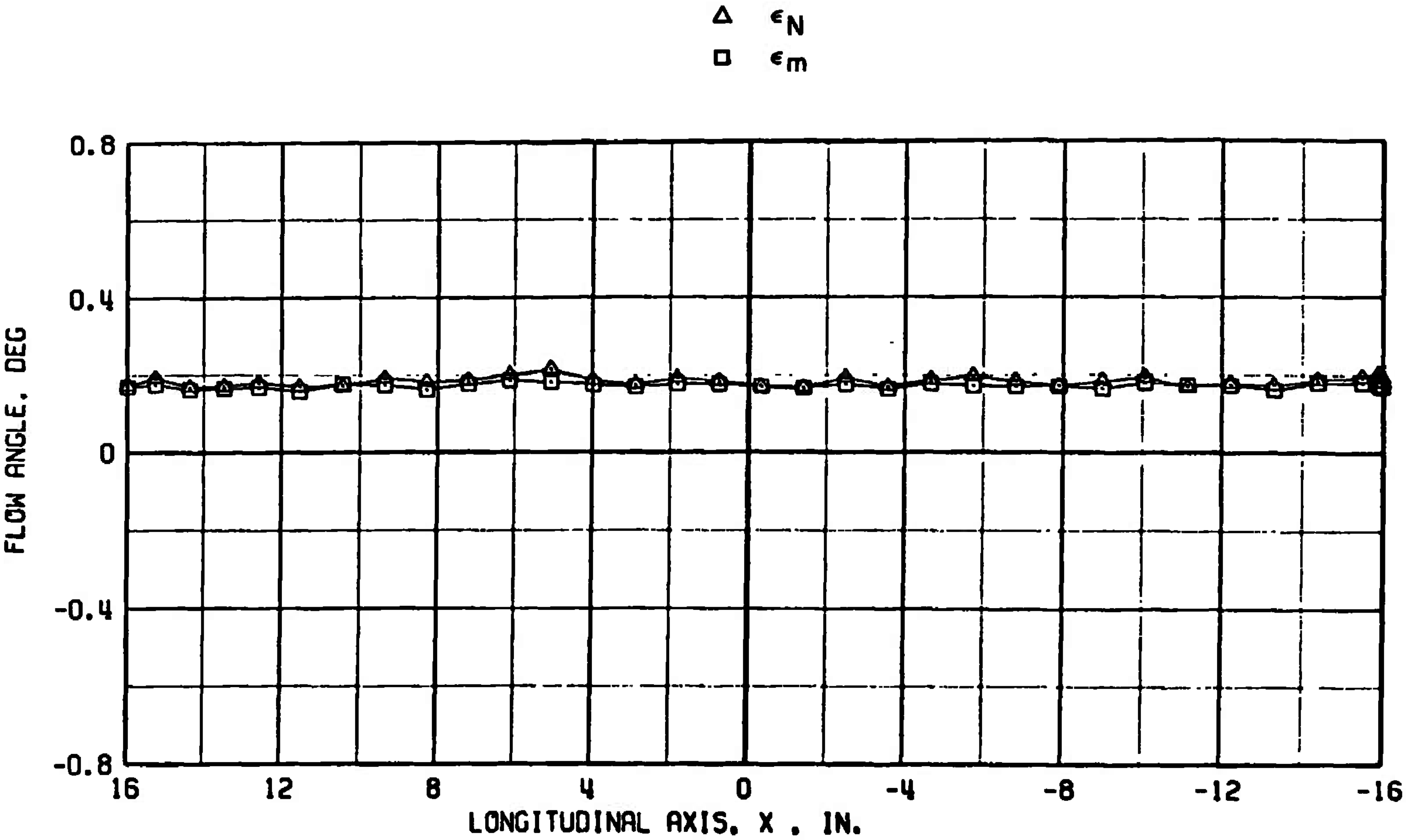

e. Y = 0, Z = 0
Figure 11. Continued.

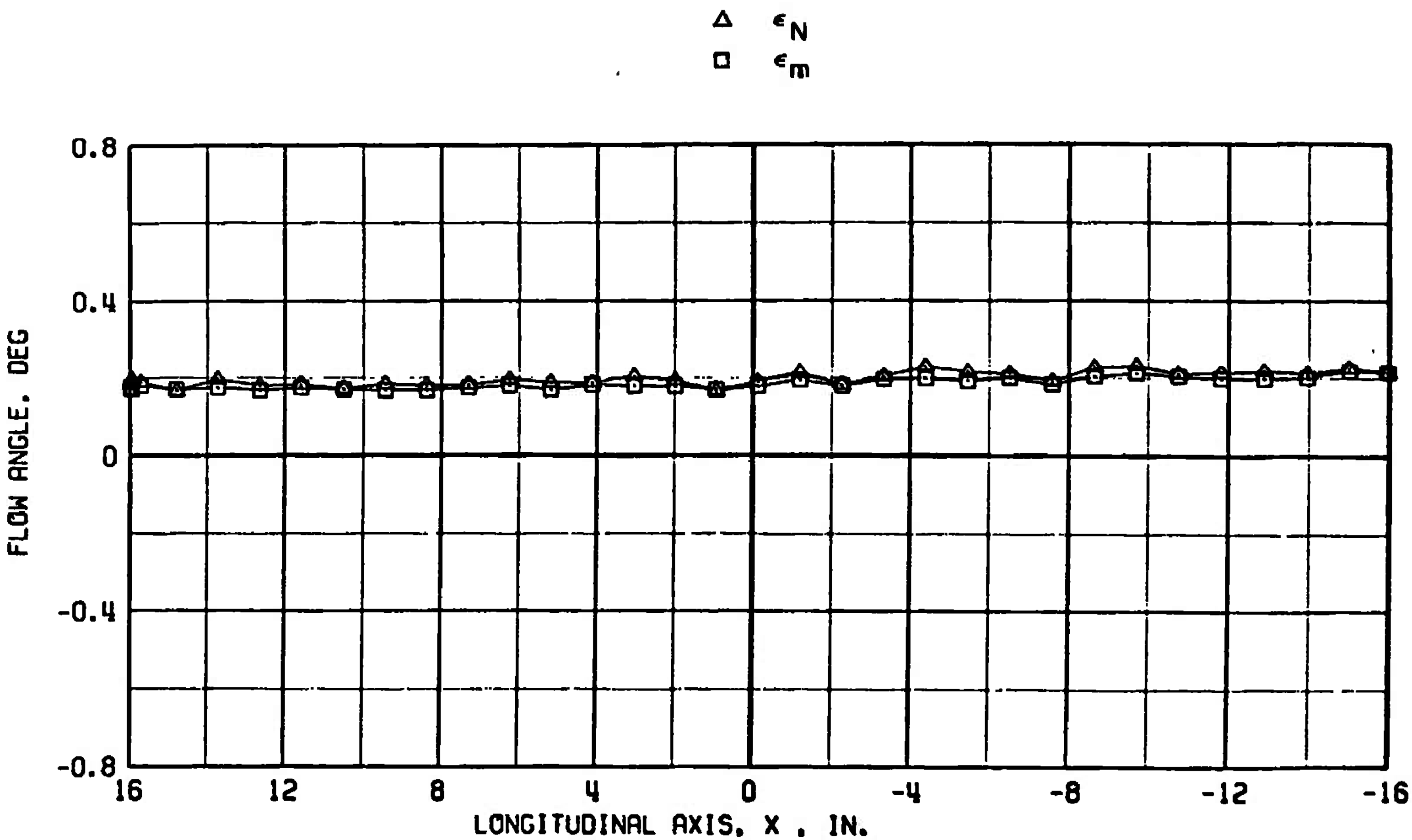

f. Y = 0, Z = 12
Figure 11. Continued.

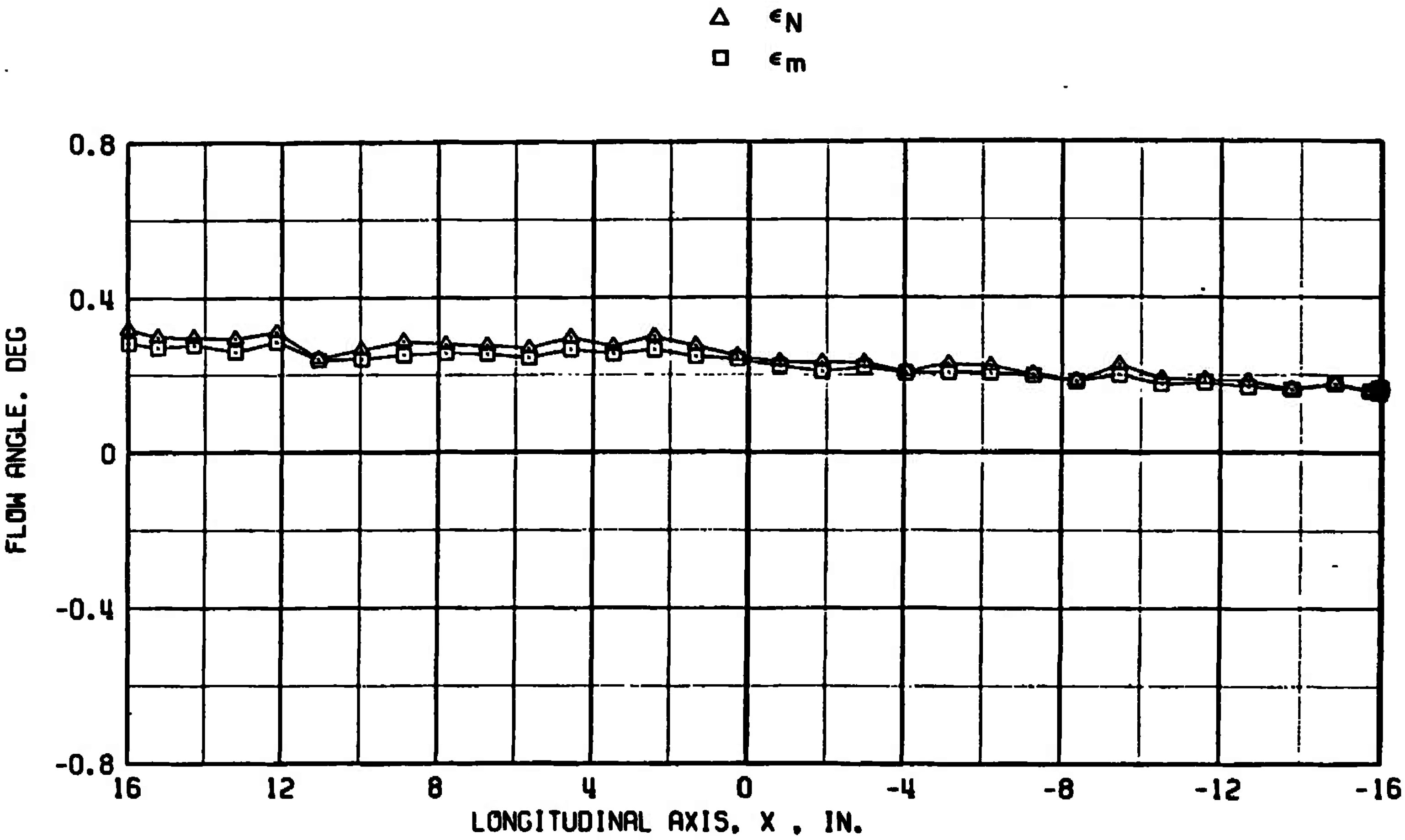

g. Y = -12, Z = -12
Figure 11. Continued.

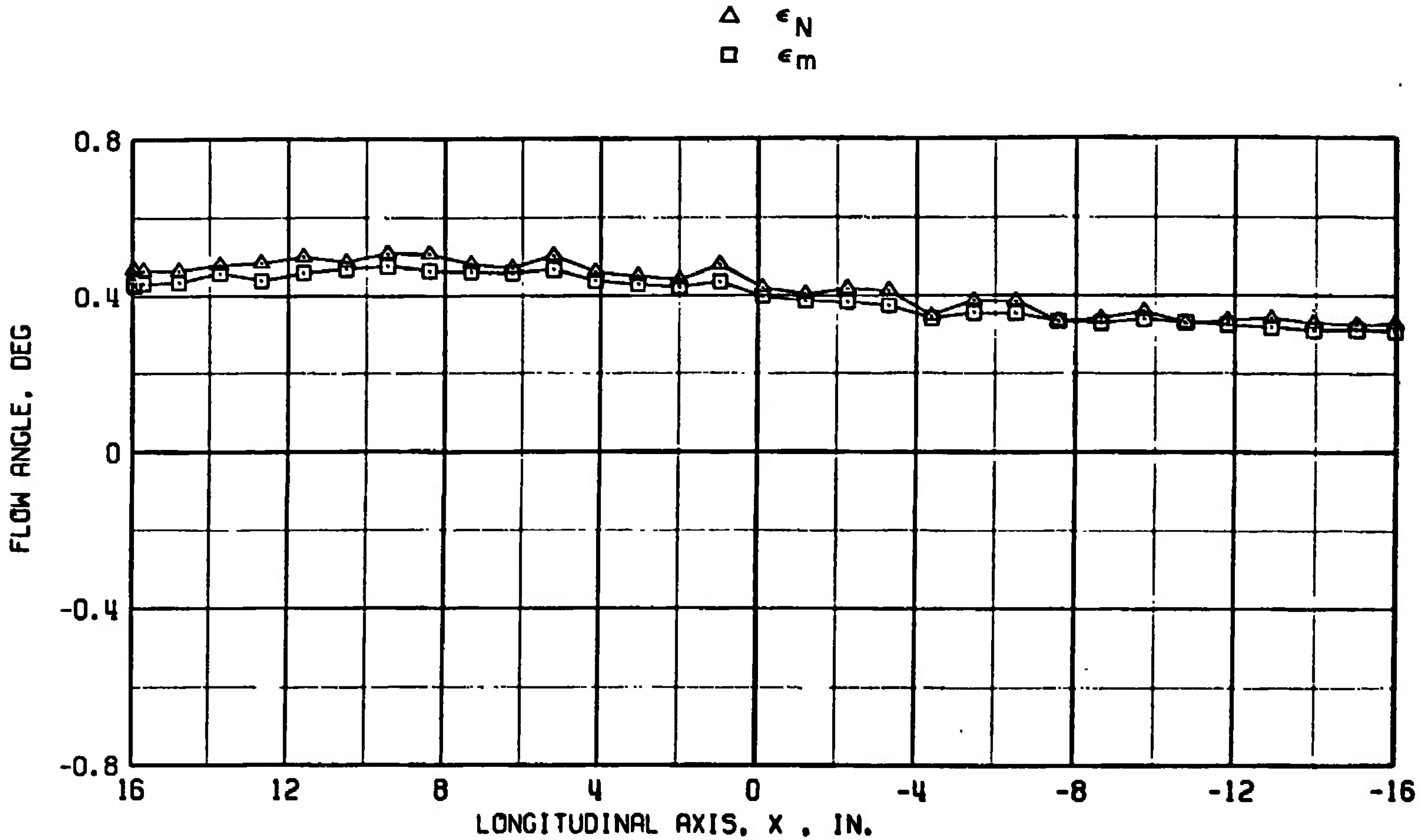

h. Y = -12, Z = 0
Figure 11. Continued.

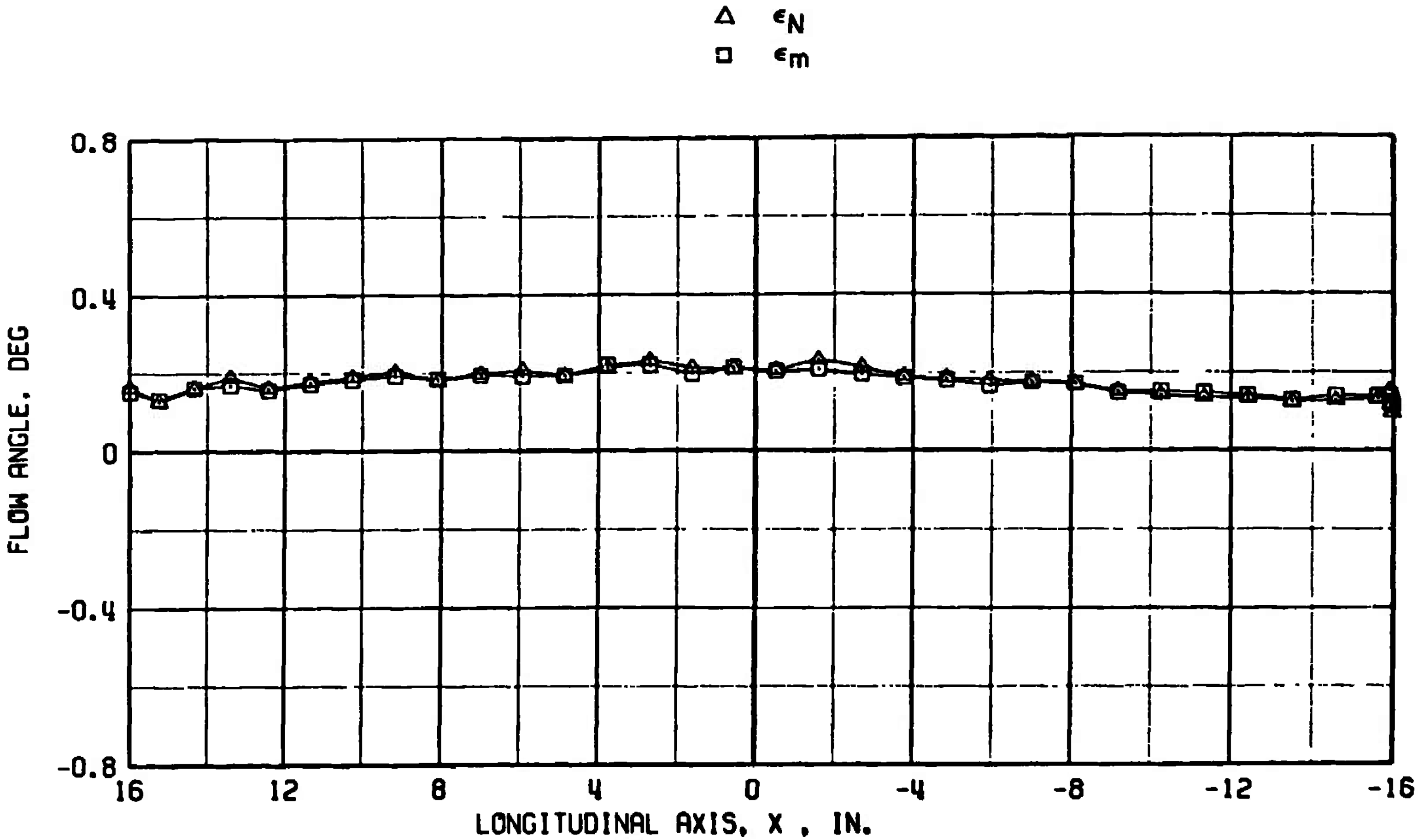

i. Y = -12, Z = 12
Figure 11. Concluded.

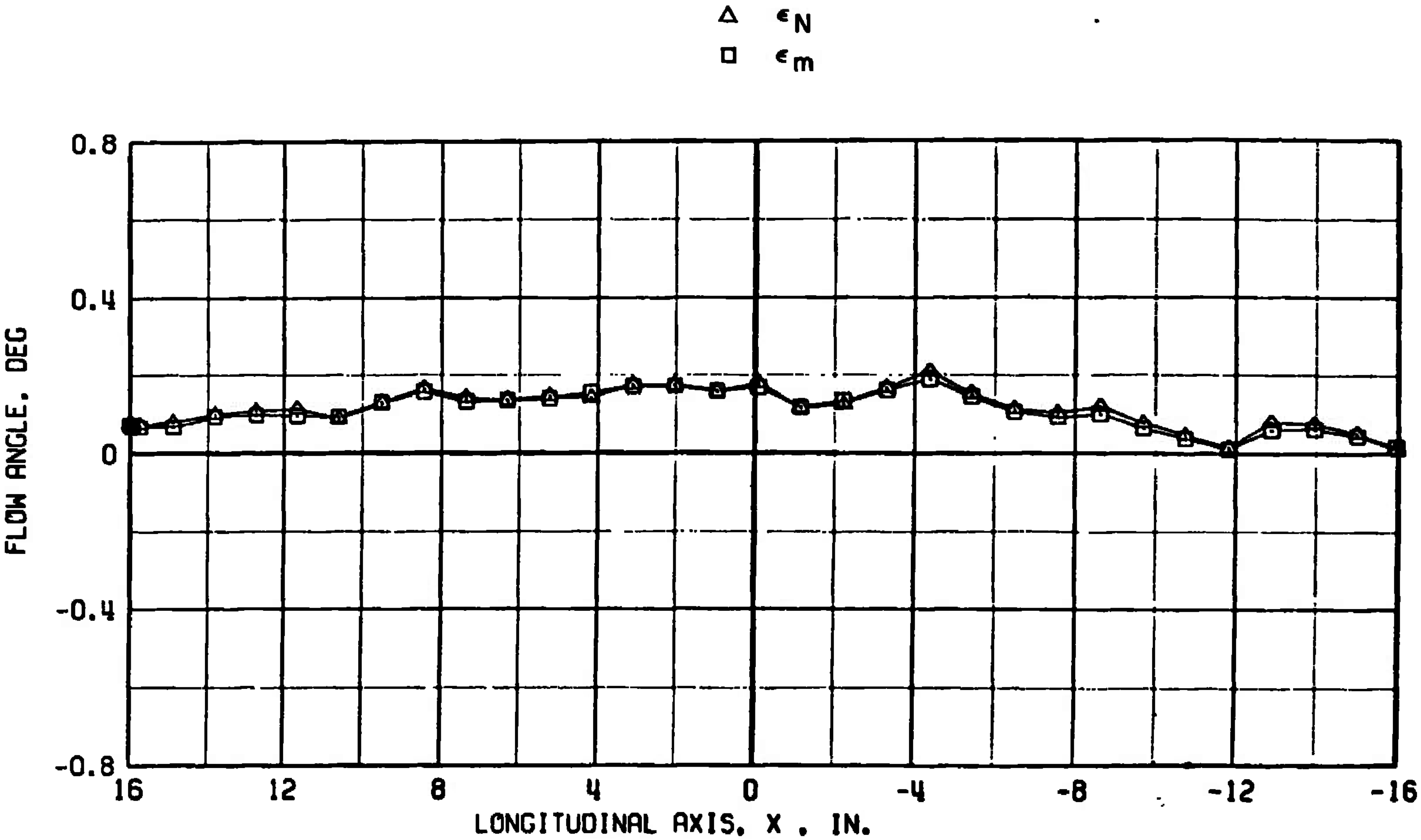

a. Pitch plane

Figure 12. Flow angle measured on the centerline longitudinal traverses at M = 1.3.

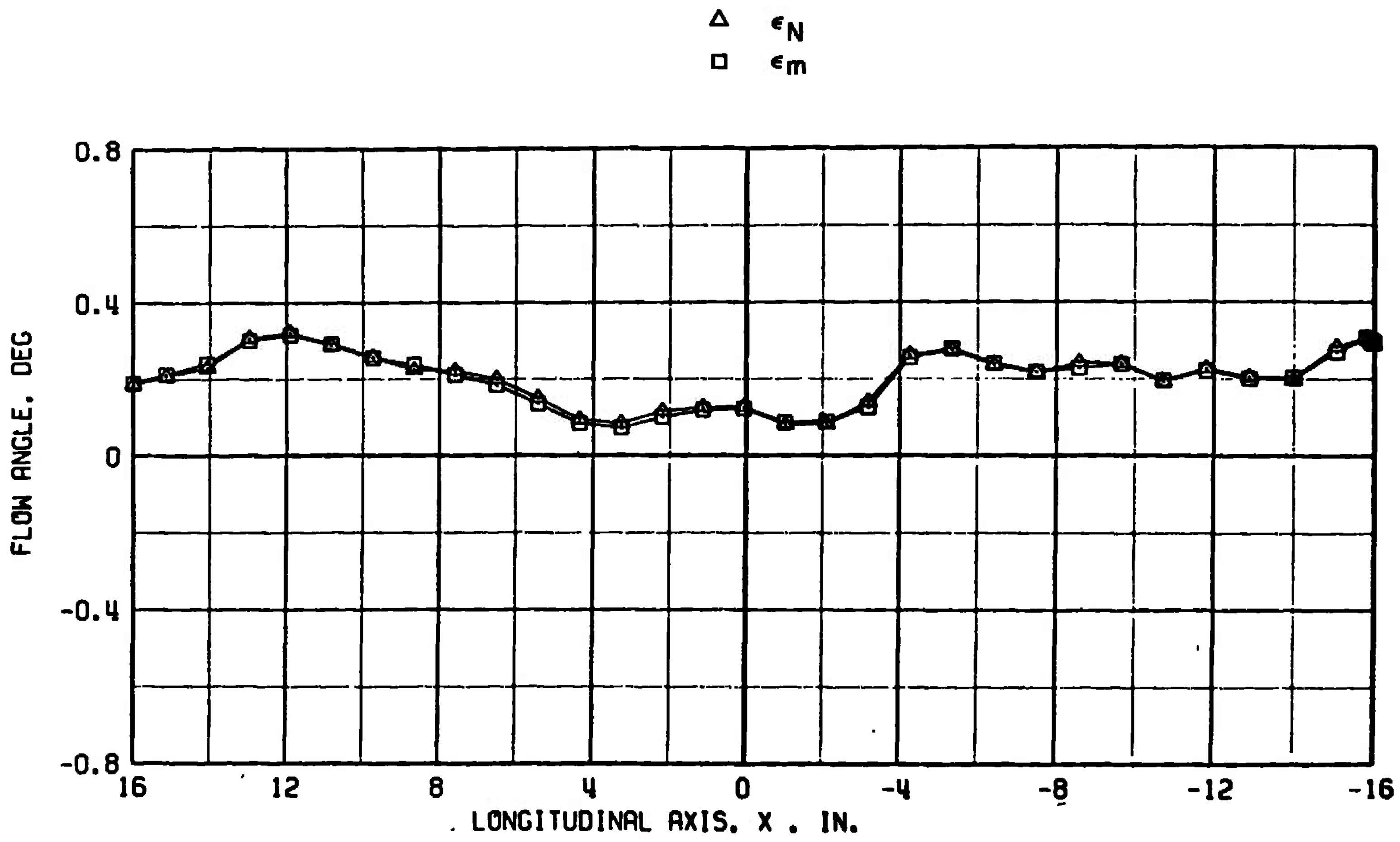

b. Yaw plane
Figure 12. Concluded.

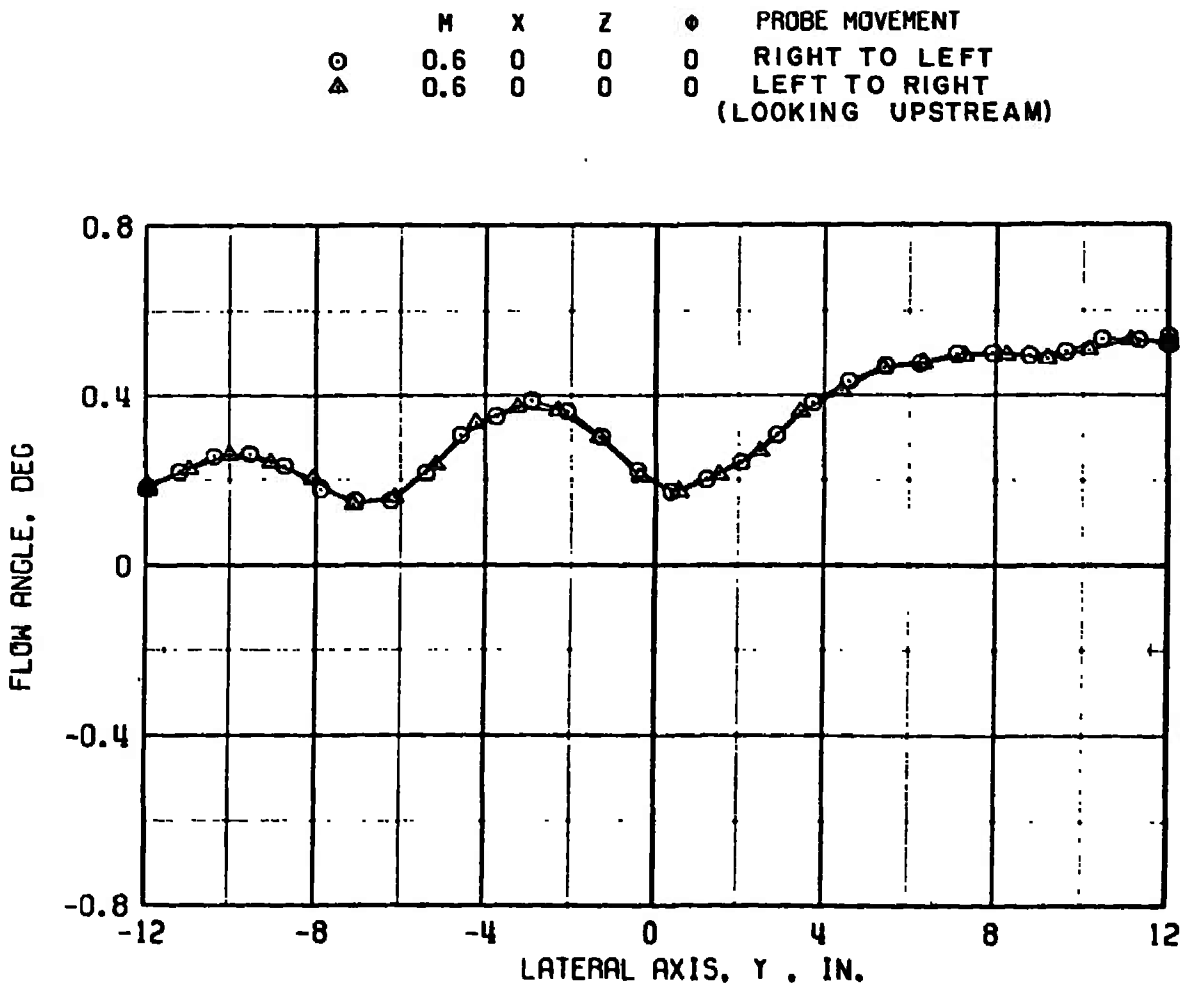

a. Pitch plane component, Y axis

Figure 13. Effect of direction of probe travel on flow angle measurement based on pitching moment.

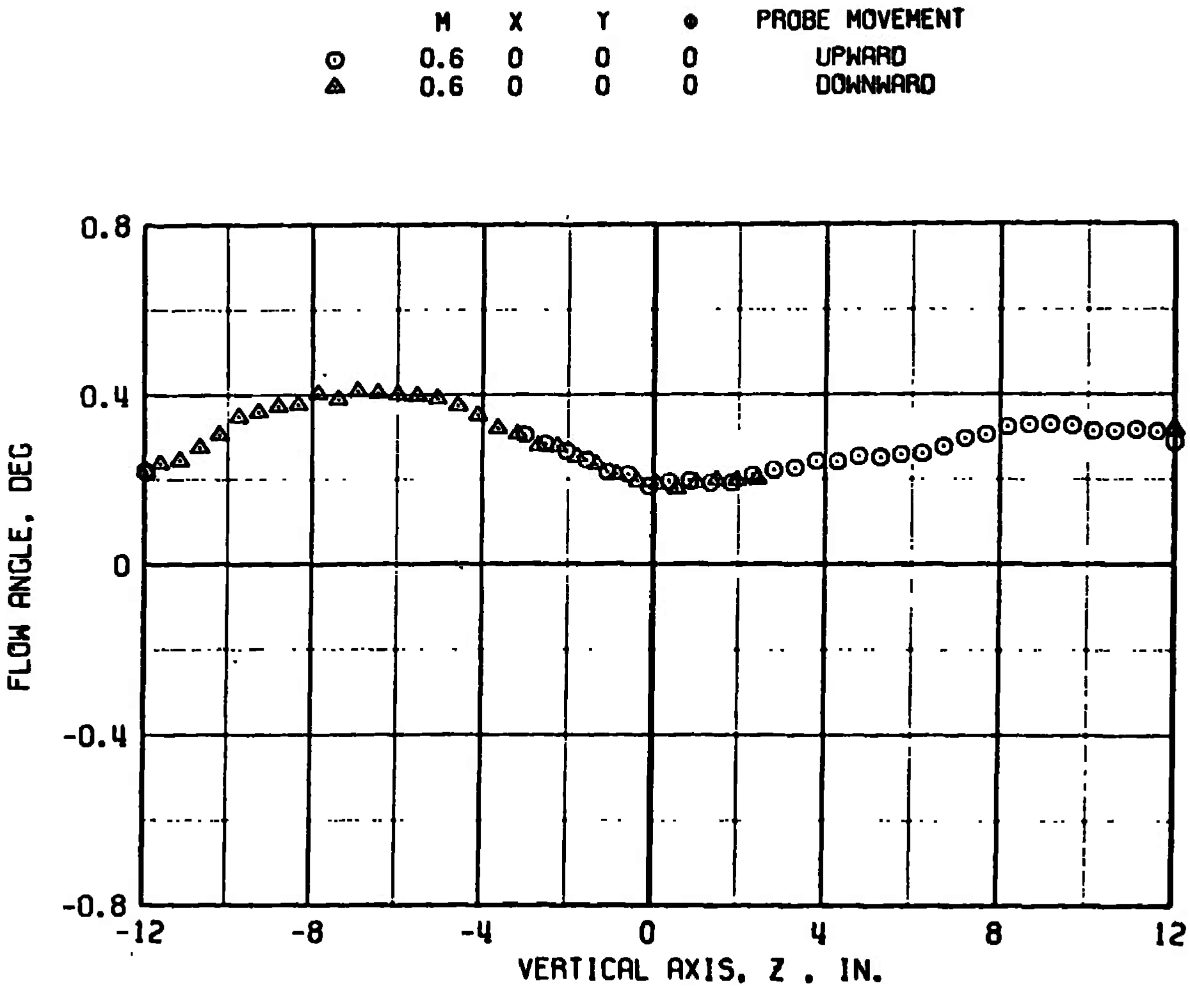

b. Pitch plane component, Z axis
Figure 13. Continued.

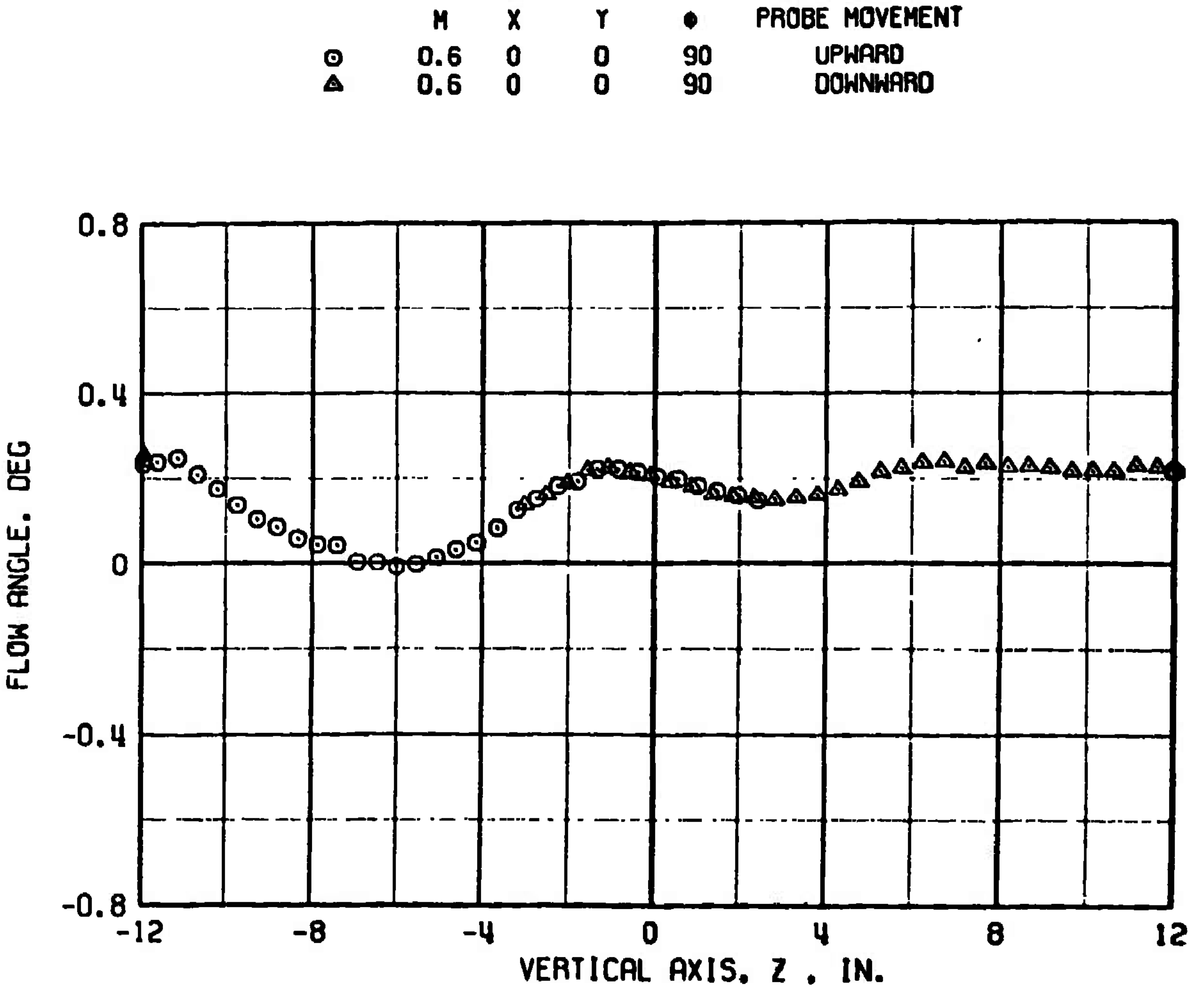

c. Yaw plane component, Z axis
Figure 13. Concluded.

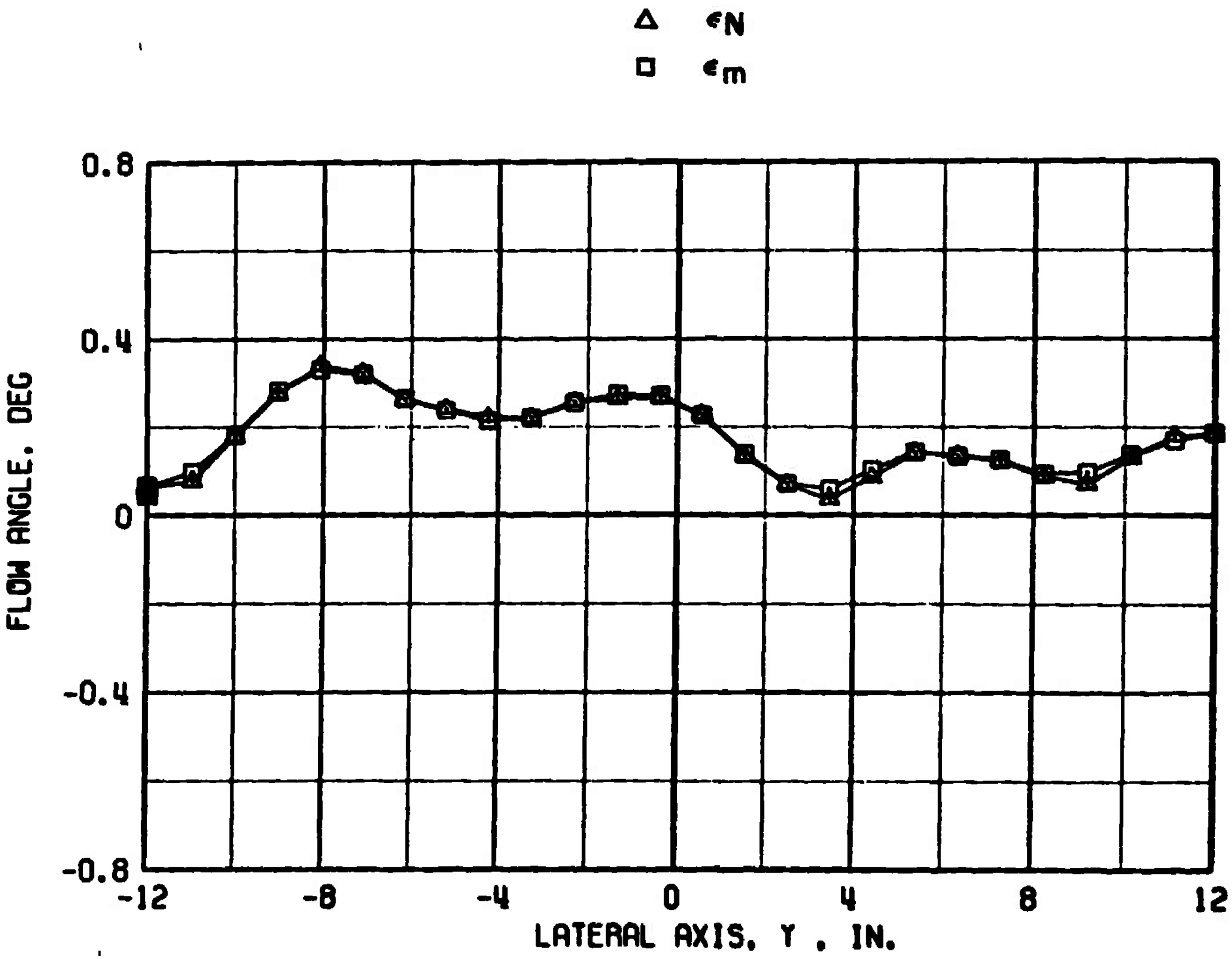

a. Six inches below the centerline

Figure 14. Flow angle in the pitch plane at X = 0, M = 0.8.

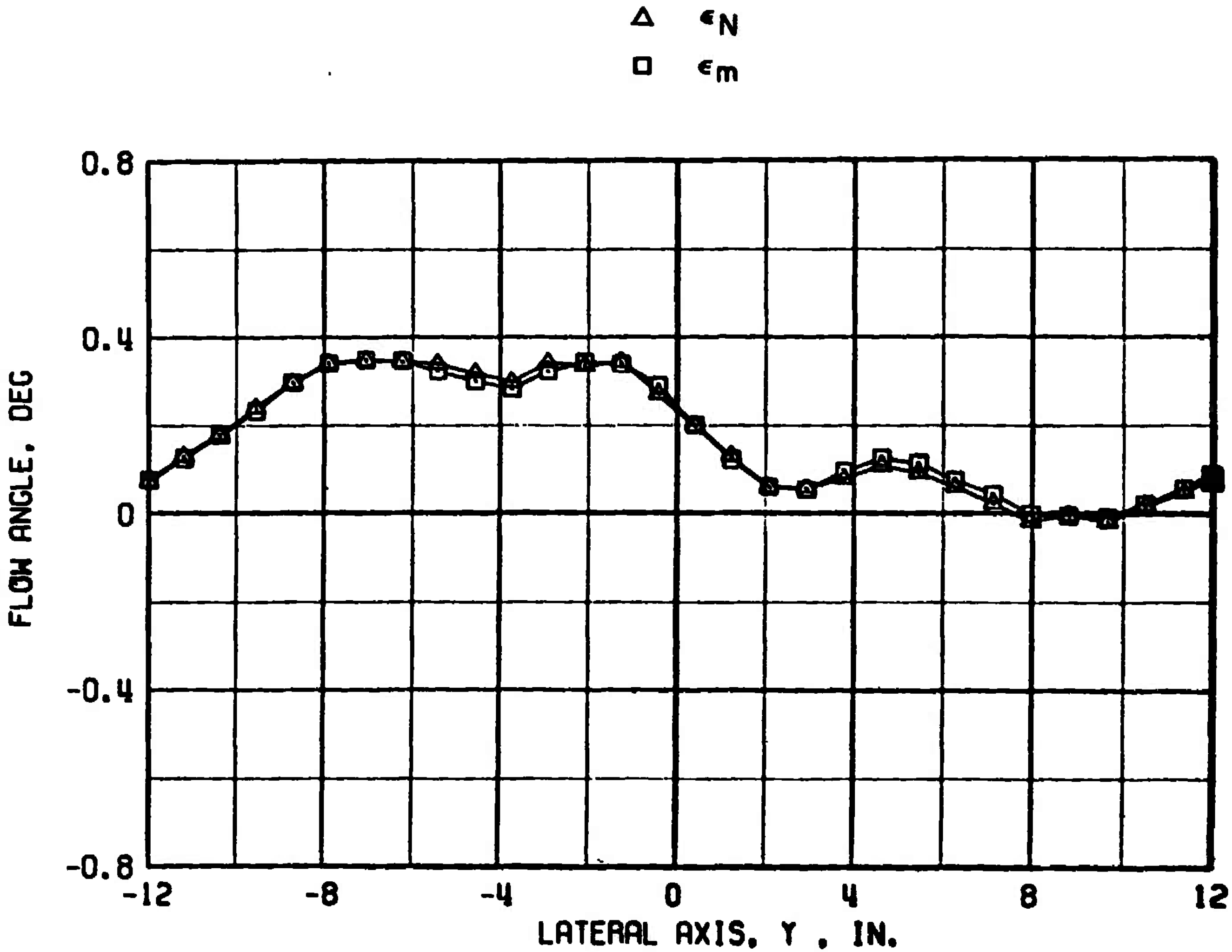

b. Nine inches below the centerline
Figure 14. Continued.

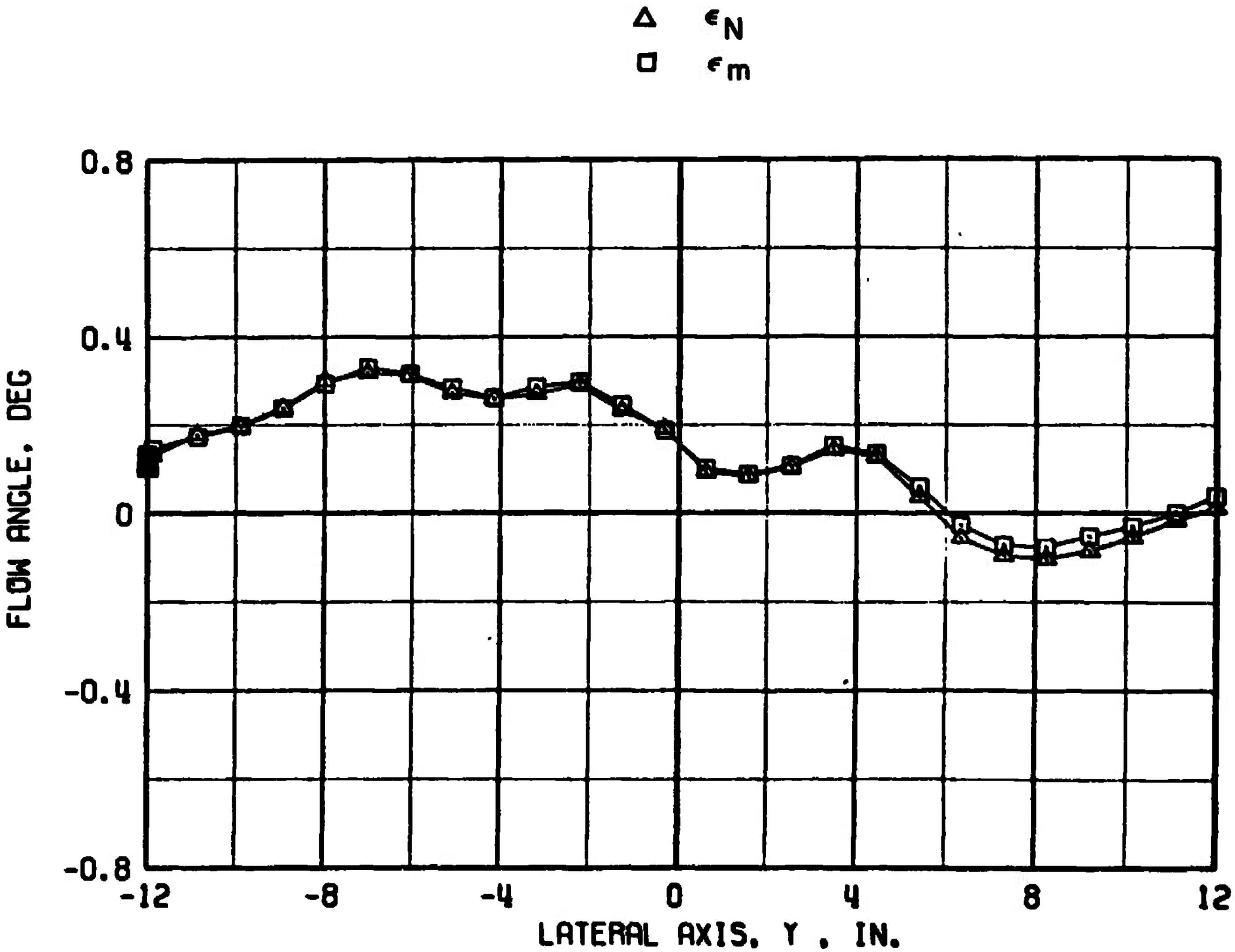

c. Twelve inches below the centerline
Figure 14. Concluded.

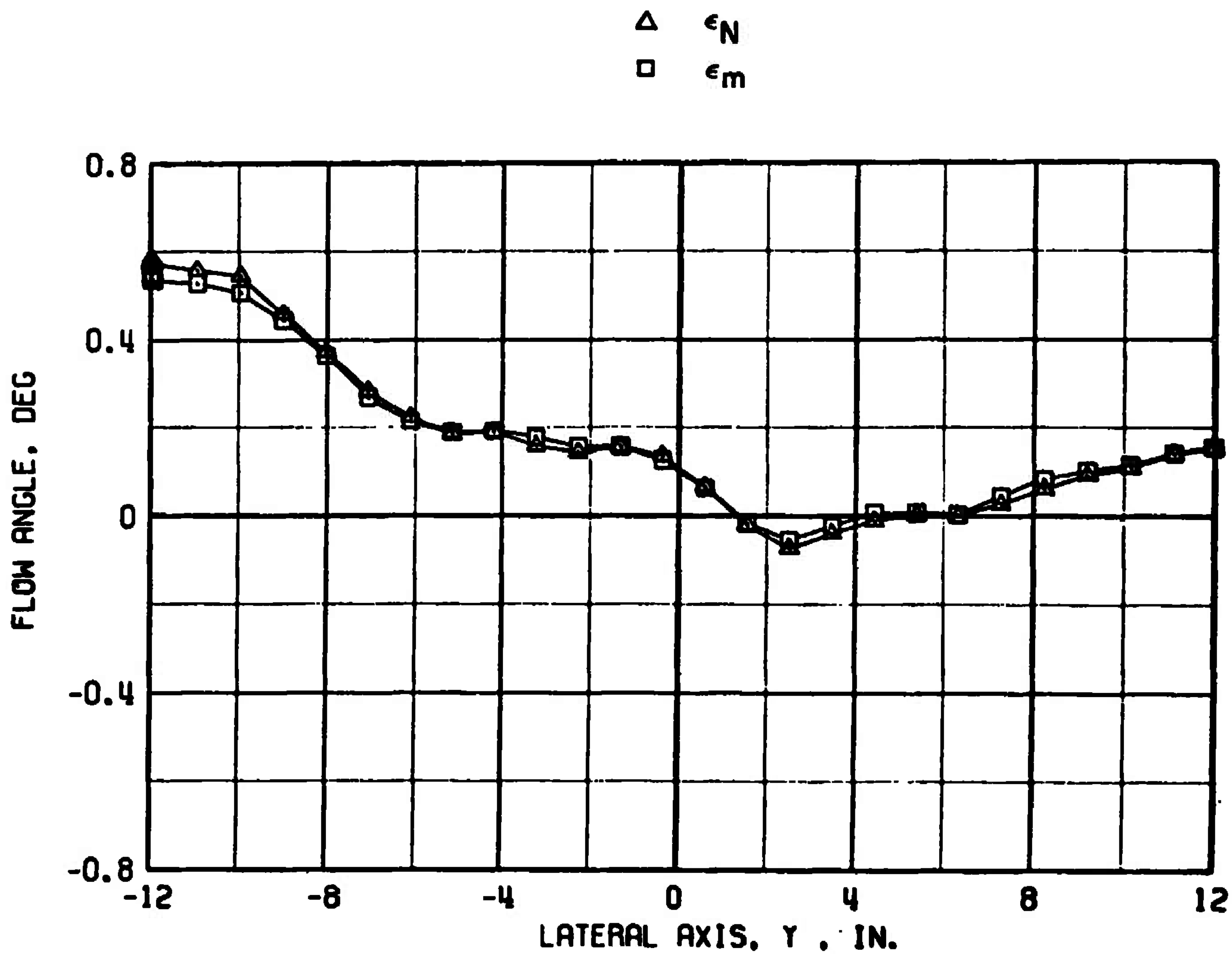

a. Three inches below the centerline
Figure 15. Flow angle in the yaw plane at X = 0, M = 0.8.

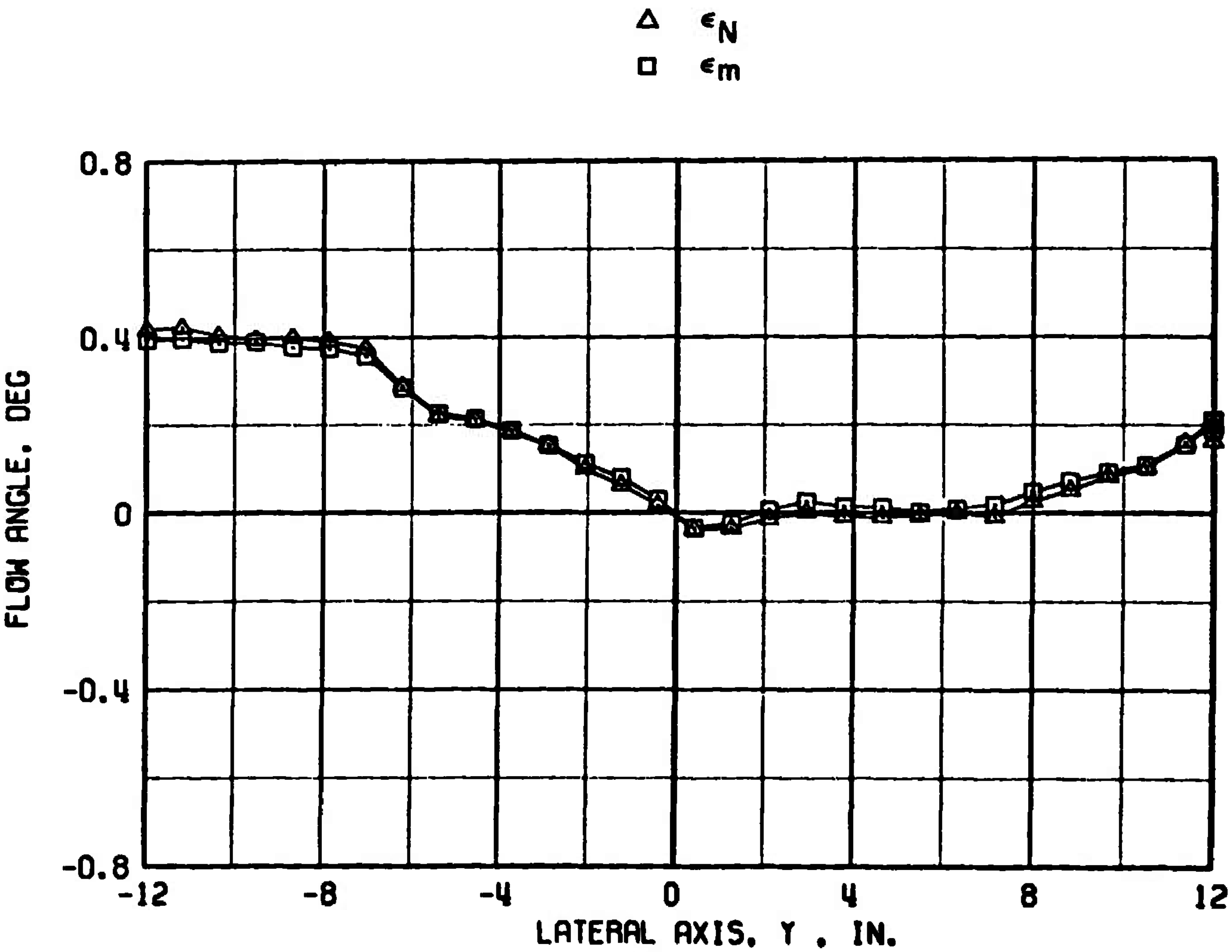

b. Six inches below the centerline
Figure 15. Continued.

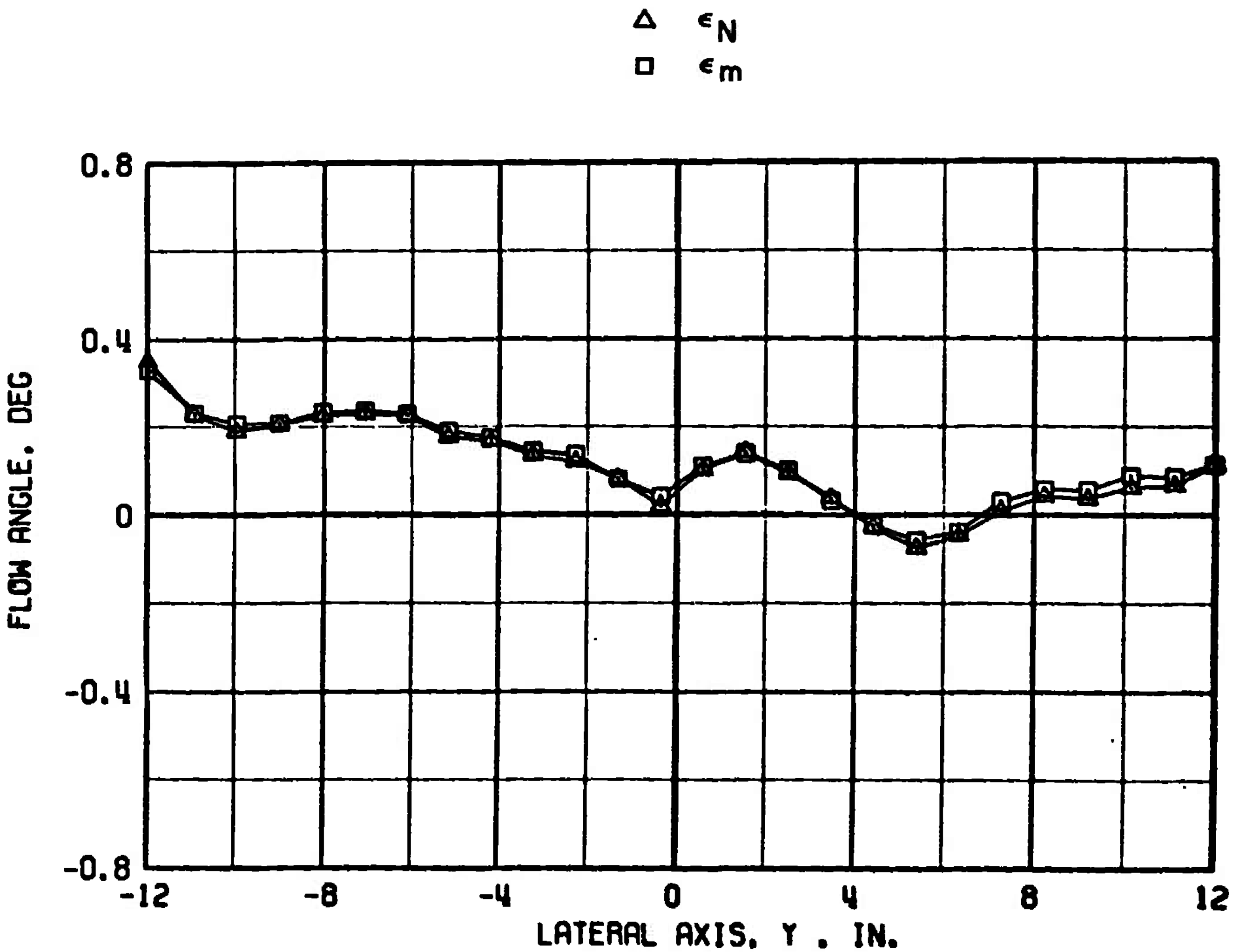

c. Nine inches below the centerline
Figure 15. Continued.

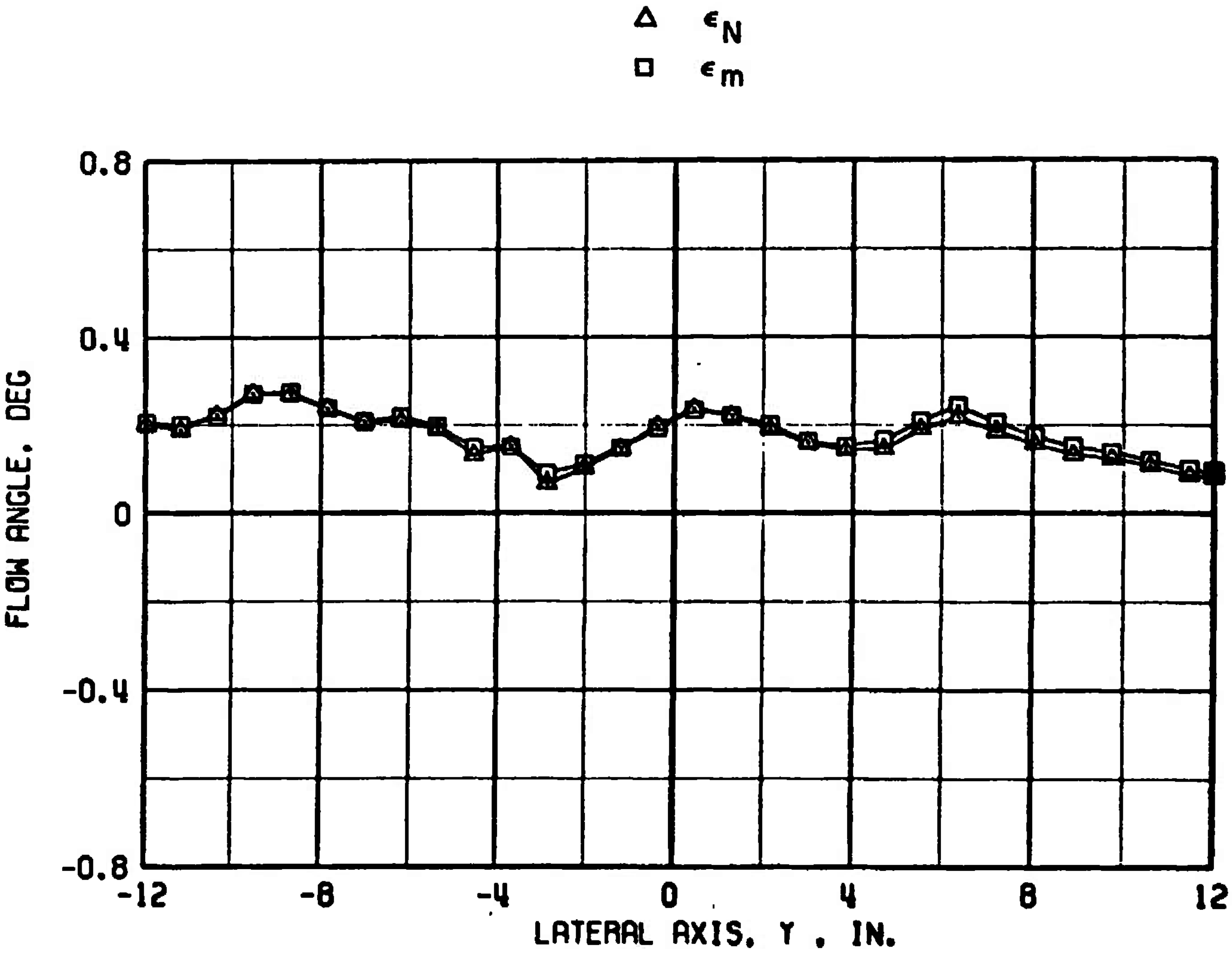

d. Twelve inches below the centerline
Figure 15. Concluded.

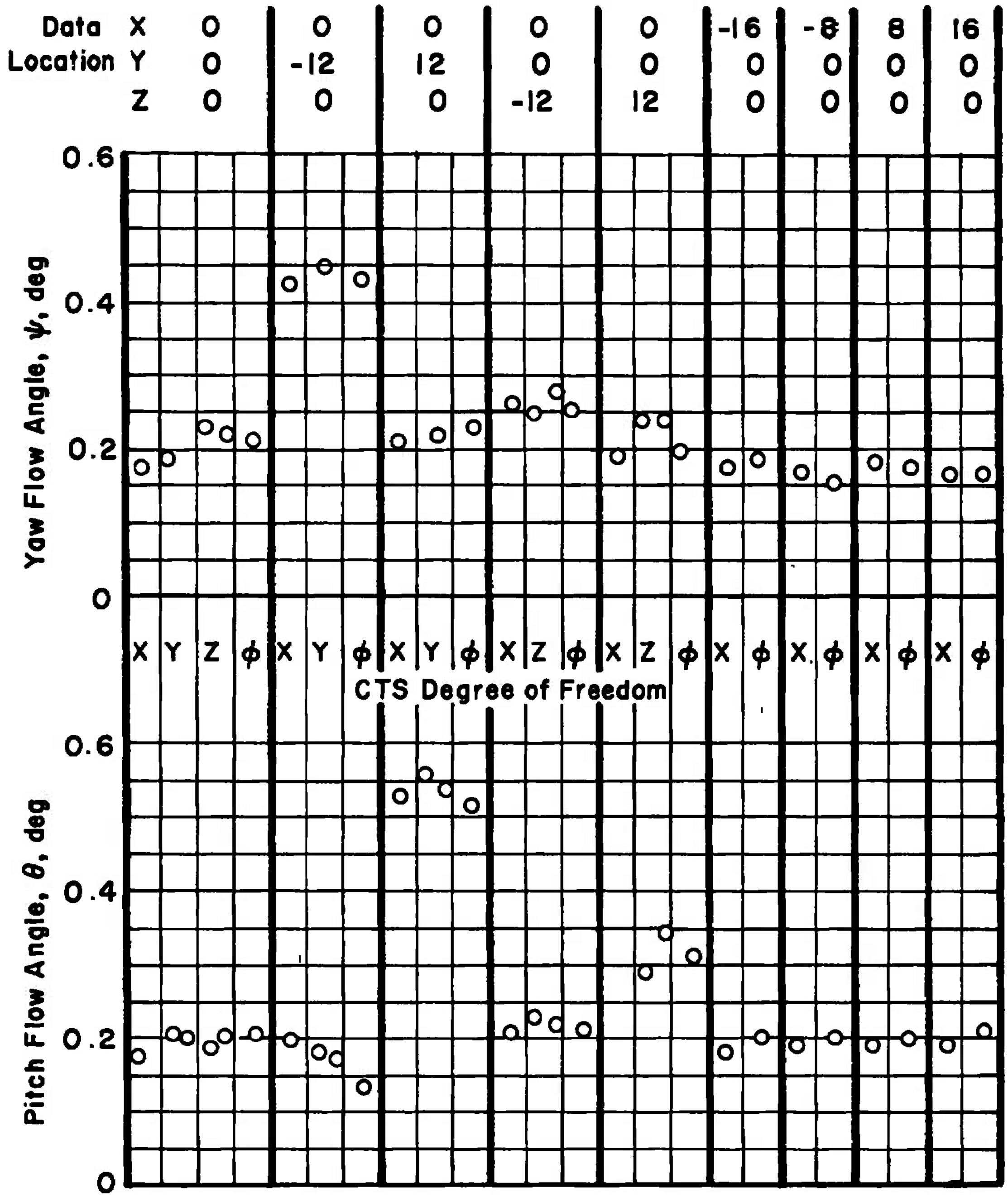

a. Normal-force data

Figure 16. Comparison of data obtained at same point during different probe motions at M = 0.6.

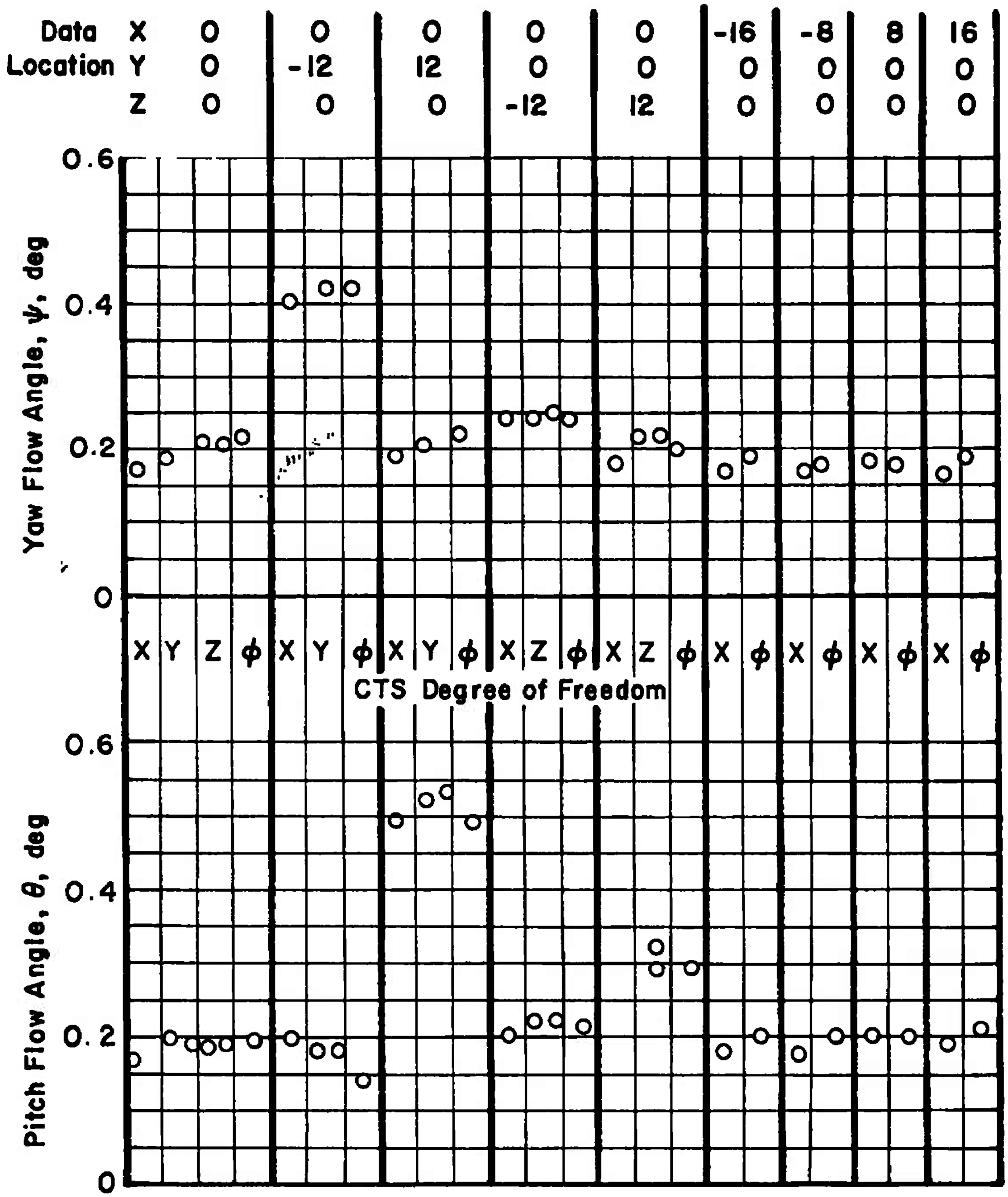

b. Pitching-moment data
Figure 16. Concluded.

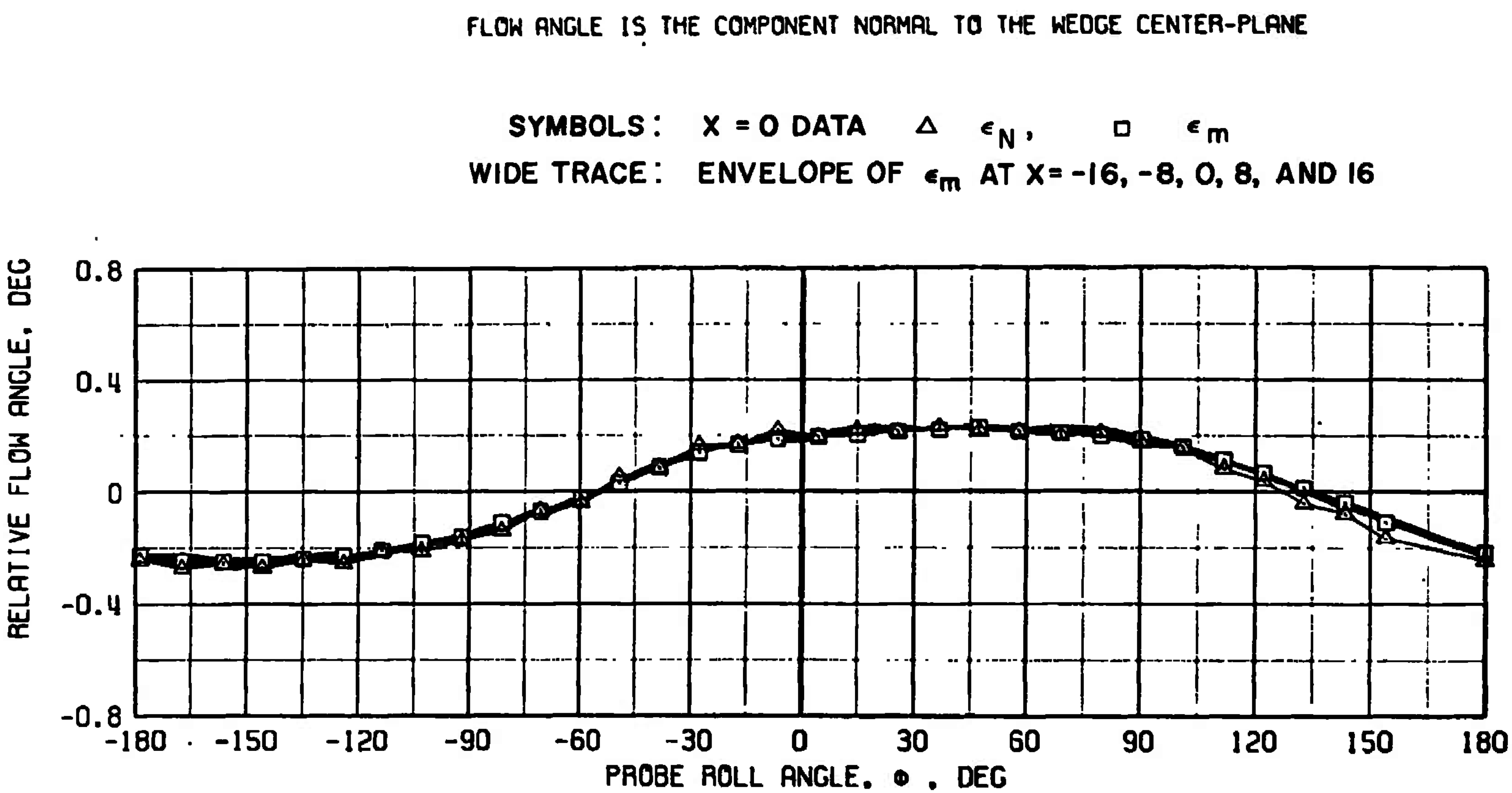

Figure 17. Data obtained during probe rolls on the centerline.

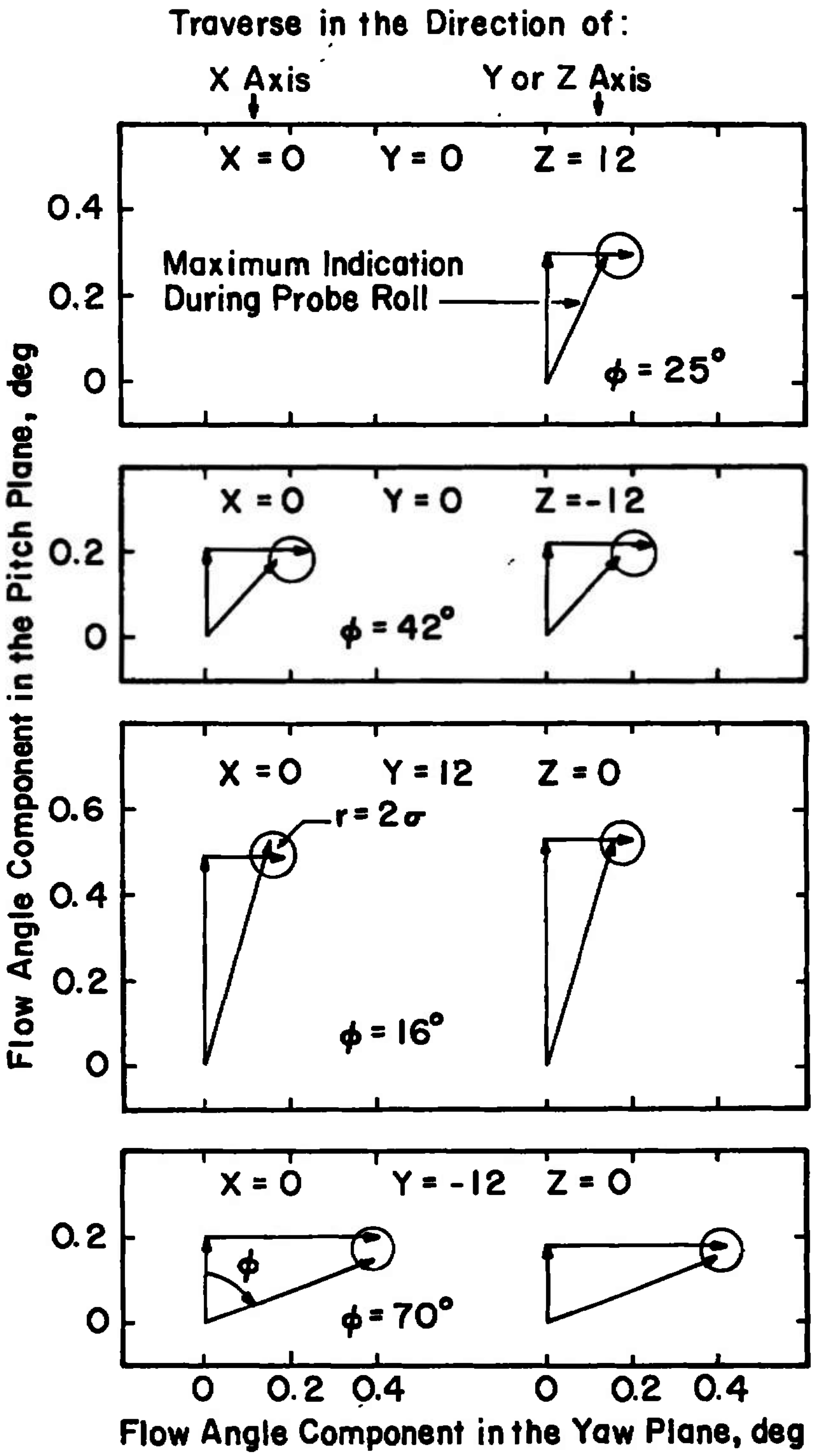

Figure 18. Direct indication of true flow angle compared with vector sum of the components at M = 0.6.

Table 1. Results of the Aerodynamic Calibrations of the Probe

Mach Number	p_t (psfa)	C_{N_θ}	$C_{N,O}$	$\theta_{F,N}$ (deg)	C_{m_θ}	$C_{m,O}$	$\theta_{F,m}$ (deg)
0.60	2000	0.08317	-0.00067	0.2517	0.4217	-0.00022	0.2562
0.60	1500	0.08514	0.00022	0.2029	0.4332	0.00569	0.2120
0.78	1200	0.08491	0.00028	0.0034	0.4245	-0.00359	0.0060
0.90	1100	0.08742	0.00030	0.0340	0.4452	-0.00635	0.0426
1.00	1100	0.08732	0.00025	0.0164	0.3946	-0.00907	0.0036
1.10	1150	0.07530	-0.00060	-0.0202	0.4047	-0.00193	-0.0248
1.30	1400	0.08467	0.00016	0.1518	0.4374	-0.00075	0.1565
1.30	1400	0.08542	-0.00007	0.1492	0.4401	-0.00297	0.1573

$X = 0 \quad Y = 0 \quad Z = 0 \quad \eta = 0 \quad \omega = 0$ and 180 deg

$$C_{N_\theta} = \frac{B - D}{2} \qquad C_{m_\theta} = \frac{F - H}{2}$$

$$C_{N,O} = \frac{A + C}{2} \qquad C_{m,O} = \frac{E + G}{2}$$

$$\theta_{F,N} = \frac{C - A}{B - D} \qquad \theta_{F,m} = \frac{G - E}{F - H}$$

Table 2. Probe Travel and Data Scan Information

Coordinate	Probe Travel	Number of Scans	Scan Interval (sec)	Probe Speed
X	32 in.	32	0.620	1.73 in./sec
Y, Right to Left*	24 in.	↓	1.528	0.55
Y, Left to Right*	↓	↓	↓	0.62
Z, Upward	↓	↓	0.364	1.29
Z, Downward	↓	↓	0.728	0.67
Roll	360 deg	↓	0.436	24.6 deg/sec
Pitch, Nose Upward	4 deg	16	0.128	1.16
Pitch, Nose Downward	↓	↓	↓	1.28
Yaw, Right to Left*	↓	↓	↓	1.36
Yaw, Left to Right*	↓	↓	↓	1.01

*Looking Upstream

Table 3. Coefficients of the Least-Squares Line Fits to the Probe Aerodynamic Calibration Data

Mach Number	A	B	C	D	E	F	G	H
0.60	-0.02161	0.08328	0.02026	-0.08307	-0.10826	0.42555	0.10782	-0.41789
0.60	-0.01704	0.08558	0.01750	-0.08470	-0.08754	0.43616	0.09609	-0.43020
0.78	-0.00008	0.08530	-0.00025	-0.08452	-0.00614	0.42588	-0.00105	-0.42308
0.90	-0.00363	0.08726	0.00231	-0.08757	-0.02534	0.44527	0.01263	-0.44532
1.00	-0.00168	0.08709	0.00118	-0.08755	-0.01049	0.39560	-0.00764	-0.39367
1.10	0.00092	0.07517	-0.00212	-0.07544	0.00810	0.40139	-0.01197	-0.40806
1.30	-0.01270	0.08460	0.01302	-0.08474	-0.06920	0.43756	0.06770	-0.43732
1.30	-0.01282	0.08499	0.01268	-0.08584	-0.07222	0.43930	0.06629	-0.44102

For the Upright Model $C_N = A + B \cdot \nu$ $C_m = E + F \cdot \nu$

For the Inverted Model $C_N = C + D \cdot \nu$ $C_m = G + H \cdot \nu$

Table 4. Confidence Limits on Random Errors in Calibration Data

Mach Number	Probe Position	$2\sigma(C_N)$	$2\sigma(C_m)$	$2\sigma(\theta_{C_N})$ (deg)	$2\sigma(\theta_{C_m})$ (deg)
0.60	Upright	±0.00478	±0.03184	±0.05752	±0.07480
0.60	Inverted	0.00250	0.01462	0.03014	0.03498
0.60	Upright	0.00322	0.02076	0.03754	0.04760
0.60	Inverted	0.00410	0.02432	0.04848	0.05650
0.78	Upright	0.00362	0.01538	0.04234	0.03610
0.78	Inverted	0.00328	0.01746	0.03876	0.04126
0.90	Upright	0.00248	0.01362	0.02850	0.03058
0.90	Inverted	0.00230	0.01470	0.02638	0.03300
1.00	Upright	0.00292	0.01262	0.03360	0.03190
1.00	Inverted	0.00264	0.01166	0.03008	0.02960
1.10	Upright	0.00154	0.01168	0.02044	0.02910
1.10	Inverted	0.00210	0.00698	0.02774	0.01712
1.30	Upright	0.00170	0.00820	0.02008	0.01874
1.30	Inverted	0.00160	0.00492	0.01890	0.01126
1.30	Upright	0.00128	0.00464	0.01506	0.01056
1.30	Inverted	0.00166	0.00564	0.01928	0.01280

APPENDIX A
DATA REDUCTION EQUATIONS

After manipulations involving balance constants and gage readouts, and retaining the standard CTS nomenclature, the data reduction equations are as follows:

$$F_{N,g} = \frac{L_5 - L_1}{1.358} \tag{A-1}$$

$$M_{m,g} = \frac{L_5 + L_1}{2} \tag{A-2}$$

where $F_{N,g}$ and $M_{m,g}$ are the total forces and moments measured by the balance, L_1 is the forward pitching moment, and L_5 is the aft pitching moment. Derivation of the following equations involves consideration of the CTS convention where a downward normal force and a nosedown pitching moment are positive.

The wedge deflection angles resulting from gross balance loads, $\Delta\nu$ in the normal-force plane and $\Delta\eta$ in the side-force plane, are

$$\Delta\nu = \{K_{\nu N}\ [F_{N,g} + W_N(1 - \cos\omega)] + K_{\nu m}\ [M_{m,g} + W_N\overline{X}_m(1 - \cos\omega)]\}\ \cos\omega \tag{A-3}$$

$$\Delta\eta = \{K_{\eta N}\ [F_{N,g} + W_N(1 - \cos\omega)] + K_{\eta m}\ [M_{m,g} + W_N\overline{X}_m(1 - \cos\omega)]\}\ \sin\omega \tag{A-4}$$

where

$K_{\nu N}, K_{\eta N}$ = Rate of deflection of the wedge in the CTS pitch and yaw planes, respectively, in terms of forces, deg/lb

$K_{\nu m}, K_{\eta m}$ = Rate of deflection of the wedge in the CTS pitch and yaw planes, respectively, in terms of moments, deg/in.-lb

W_N = Static tare weight of the wedge as measured by balance normal force, lb

$\overline{X}_m$ = Distance along the balance X-axis between the wedge center-of-gravity position and the effective pitching-moment center of the balance, in.

ω = Angular displacement of the wedge from the upright horizontal position in roll, deg

The components of the angular displacement of the wedge-balance axis from parallelism with the centerline, ν in the pitch plane and η in the yaw plane, are

$$\nu = \nu_i + \Delta\nu \tag{A-5}$$

$$\eta = \eta_i + \Delta\eta \tag{A-6}$$

where the subscript i denotes the value given by the CTS rig angle indicators.

Static tares are calculated from

$$F_{N,st} = W_N \ (1 - \cos\nu \cos\omega) \tag{A-7}$$

$$M_{m,st} = \overline{X}_m \ F_{N,st} \tag{A-8}$$

and the probe aerodynamic coefficients are given by

$$C_N = \frac{F_{N,g} + F_{N,st}}{qS} \tag{A-9}$$

$$C_m = \frac{M_{m,g} + M_{m,st}}{qS\overline{C}} \tag{A-10}$$

where the wedge reference area (S) is 0.04247 ft^2, the reference length $(\overline{C})$ is 1 in., and q is the dynamic pressure of the tunnel flow.

The calibrations were accomplished using the above equations in conjunction with the standard tunnel measurements and standard curve fitting procedures. Constants found during the calibrations, defined in the text nomenclature using more generally understood symbolism, were used to determine the component of tunnel flow angle normal to the wedge centerplane as follows:

$$\epsilon_N = \frac{C_{N,o} - C_N}{C_{N\theta}} + \nu \cos\omega + \eta \sin\omega \tag{A-11}$$

$$\epsilon_m = \frac{C_{m,o} - C_m}{C_{m\theta}} + \nu \cos\omega + \eta \sin\omega \tag{A-12}$$

Epsilon is defined as the component of flow angle in the pitch plane or the yaw plane when $\omega = 0$ or 90 deg, respectively. When ω has any other value, it is simply the component normal to the centerplane of the wedge.

NOMENCLATURE

A	Intercept on the C_N axis of the straight line fitted to the probe-upright, normal-force, calibration data
B	Slope of the straight line fitted to the probe-upright, normal-force, calibration data, deg^{-1}
C	Intercept on the C_N axis of the straight line fitted to the probe-inverted, normal-force, calibration data
C_m	Pitching-moment coefficient
$C_{m,o}, C_{N,o}$	Probe asymmetry corrections
$C_{m\theta}$, $C_{N\theta}$	Probe sensitivity to flow angularity, deg^{-1}
C_N	Normal-force coefficient
D	Slope of the straight line fitted to the probe-inverted, normal-force, calibration data, deg^{-1}
E	Intercept on the C_m axis of the straight line fitted to the probe-upright, pitching-moment, calibration data
F	Slope of the straight line fitted to the probe-upright, pitching-moment, calibration data, deg^{-1}
G	Intercept on the C_m axis of the straight line fitted to the probe-inverted, pitching-moment, calibration data
H	Slope of the straight line fitted to the probe-inverted, pitching-moment, calibration data, deg^{-1}
M	Mach number
p_t	Stagnation pressure, psfa
X, Y, Z	Coordinate axes, in. Positives are upstream, toward left wall (looking upstream), and upward, respectively. Zeros are set with probe axis on tunnel centerline and probe leading edge at tunnel station 108.

ϵ	Flow angle component normal to the wedge center plane, deg, positive when flow impinges on wedge center plane from side opposite the $\omega = 0$ upper surface
θ	Flow angle component in pitch plane, deg, positive upward
θ_F	Flow angle at location of probe for calibration, as defined in Fig. 6
ν, η, ω	Angular displacement of the CTS sting in pitch, yaw, and roll, respectively, deg. Positives are nosedown, to the left looking upstream, and clockwise, respectively
σ	Standard deviation
$2\sigma(i)$	Twice the standard deviation (considered equal to the confidence limits on random errors in parameters for which an error analysis of data from this test has been made)
ϕ	Probe roll angle, deg, positive clockwise looking upstream
ψ	Flow angle component in the yaw plane, positive toward right wall looking upstream, deg

SUBSCRIPTS

m	Based on calculation of pitching moment
N	Based on calculation of normal force